XI 11

Feb 1964

DYNAMIC PROBLEMS IN LAUNCH VEHICLES AND SPACECRAFT

by

Robert M. Hunt, Staff Scientist, MSFC, Huntsville, Alabama
and
Francis C. Hung, Director of Dynamic Sciences, S&ID,
North American Aviation, Inc., Downey, California

With the advent of manned space flight, heavier emphasis must be placed on reliability, crew safety, and mission success. These goals must be realized with accompanying minimum weight design and minimum cost. Requirements for a successful space flight demand among other things a thorough knowledge of the dynamic problems in launch vehicles and spacecraft.

Increases in the vehicle size, launch thrust, and re-entry speed increase the severity of interaction of the vehicle structure, contained fluids, and subsystems. For preliminary design purposes this interaction may be approximated from past performance, rough estimates, and simple idealizations. However, such rough predictions or estimates must be followed by rigorous long-term research so that all phases of this interaction process are investigated. Unfortunately these long term studies which help to prevent flight failures are difficult both to plan and to finance. When difficulties are encountered in such a problem, quite often the fast and simple "fix" resorted to for expediency may penalize future projects, since adequate research into the problem has not been accomplished.

Since dynamic problems in launch vehicles and spacecraft so vitally affect their reliability, and since the reliability of our vehicles involve our national prestige, more long-term research into structural dynamics is necessary. Some of these dynamic problems are:

1. Crawler-transport-vehicles dynamics
2. Ground wind during pre-launch and launch
3. Acoustic environment at launch
4. Vehicle response to acoustic environment
5. Thrust build-up structural transient
6. On pad abort structural transient
7. Launch release structural transient
8. Acoustic and buffeting environment in flight
9. Coupling of engine and vehicle dynamics
10. Vapor-liquid and bulkhead interaction during engine cutoff transient
11. Separation of stages or shrouds (jettisoning)
12. Dynamics of fluids under low-g environment
13. Rendezvous and docking
14. Stabilization of space station with cable-connected configurations
15. Aeroelasticity effects of inflatables
16. Impact of spacecraft in water
17. Impact of spacecraft of shell configuration on land
18. Lunar landing structural dynamics

1. Crawler-Transport-Vehicle Dynamics

An examination of the natural vibration characteristics of the pre-launch configuration (i.e., the Saturn V, the launch platform and the umbilical tower) is warranted in view of

1) the transient dynamic behavior induced during the crawler-transportation phase of the pre-launch operation,
2) the transient dynamic behavior induced by ground winds, and
3) the transient dynamic behavior induced by engine start-up, and in the case of abort, engine cut-off and rebound.

The completely assembled pre-launch configuration, shown in Figure 1, consists of the 350-ft Saturn V, the two-story, 2,000-ton launch platform, and the 400-ft, 750-ton umbilical tower. The configuration is moved to the launch pad by a crawler-transporter over a distance in excess of two miles at roughly the speed of one mile per hour. Four hydraulic cylinders maintain the level of the load on the crawler-transporter to within 10 minutes of arc.

At the launch pad, which consists essentially of a concrete foundation housing the flame deflector, the launch platform is secured by six steel pedestals and four extendable columns. (See Figure 2.) The stay-time at the launch site is approximately one week.

The structural integrity of the Saturn V during the pre-launch and launch operations depends on, in addition to other considerations, its dynamic compatibility with the launch platform and the umbilical tower.

The natural vibration characteristics of the pre-launch configuration should be such that no adverse interaction with the dynamic behavior of the crawler-transporter occurs during the trip to the launch site and, in the event of storm

warnings, return to the vertical assembly building. These characteristics also should reflect no severe dynamic load amplification or critical fatigue loads due to unsteady ground winds during the stay-time at the launch site. The crawler transport system is being developed by the Kennedy Space Center.

The capability of adjusting the natural vibration characteristics of the pre-launch configuration augments the flexibility of the mobile launcher concept. The natural frequency and the damping can be changed appreciably by using the umbilical service arms as structural ties between the Saturn V and the umbilical tower. Since local overstressing of the Saturn V may cause more harm than the imposed environmental load, all eight of the service arms cannot be used as structural ties. Moreover, it is apparent that each service arm used in this manner will have attachments which are consistent with the local Saturn V structure.

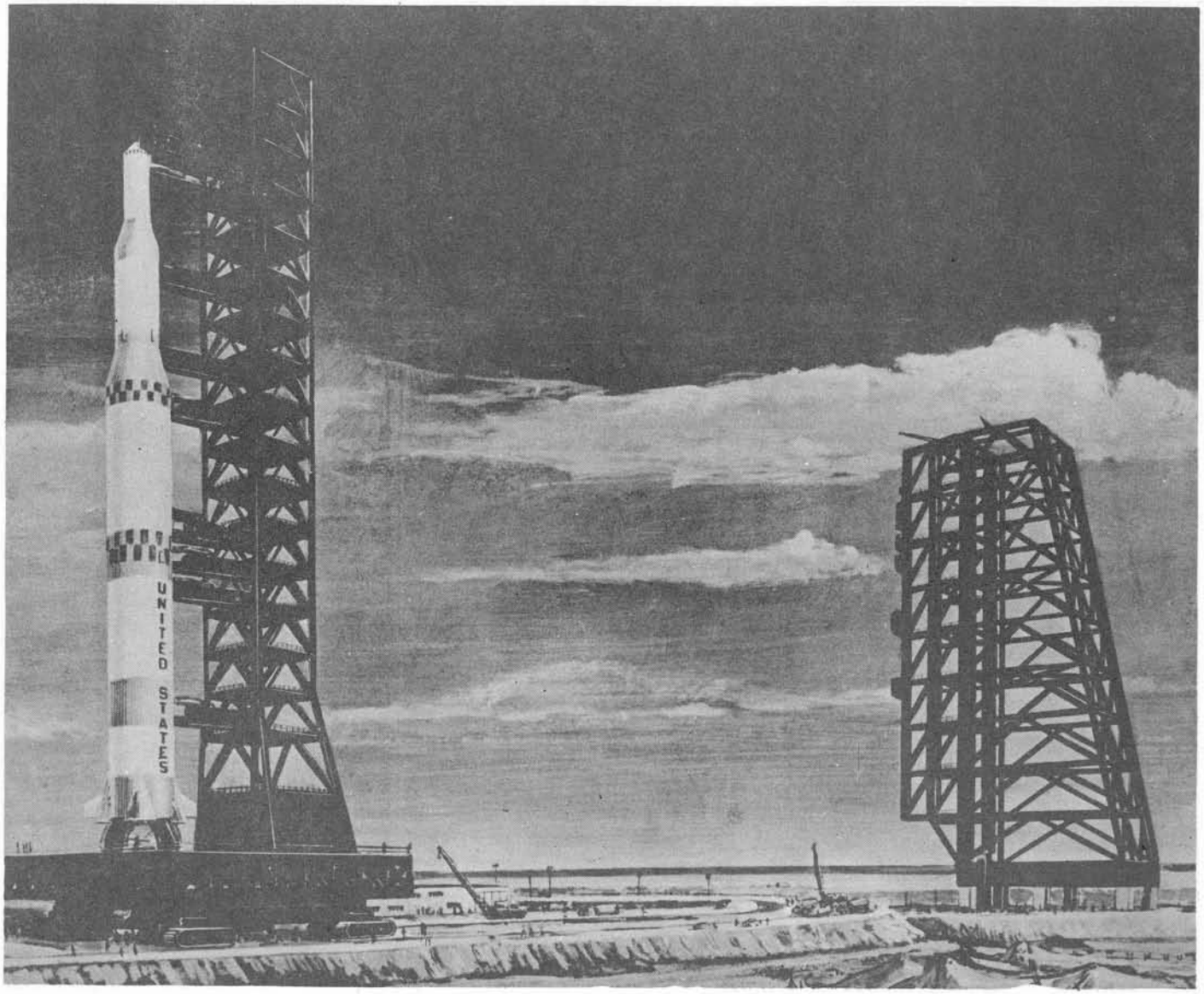

Figure 1. Saturn V Pre-Launch Configuration

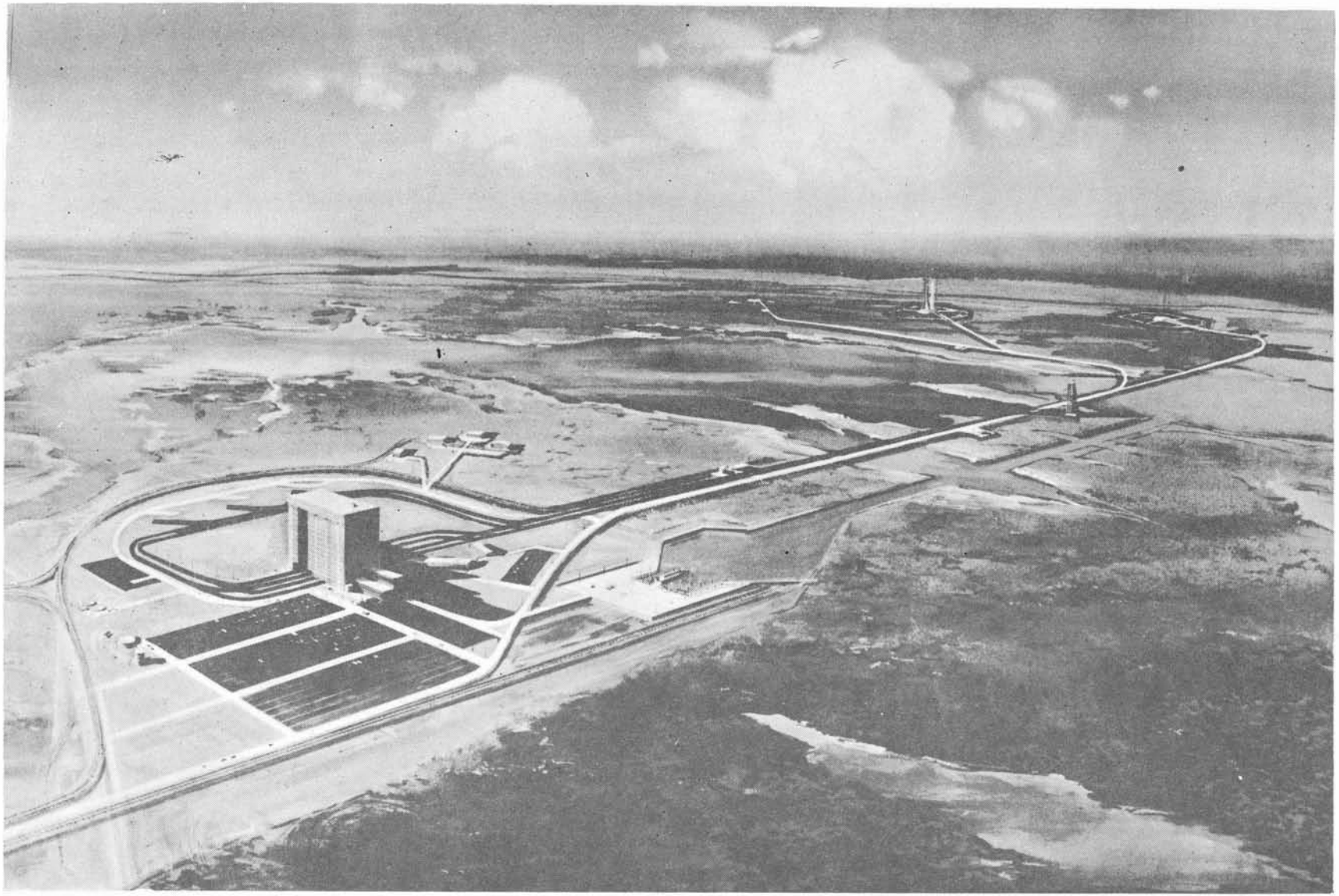

Figure 2. Advanced Saturn Launch Complex 39

2. Ground Wind During Pre-Launch and Launch

Resonant loading conditions encountered during recent NASA-Langley ground wind tests of the Saturn V scale model have emphasized the uncertainty of test results obtained without full-scale Reynolds Number simulation. This resonant condition translated to the full-scale vehicle would occur at approximately 40 ft/second. At this velocity, the full-scale Reynolds Number would be approximately twice that for the resonant condition during the test. (See Figures 3 and 4.)

Furthermore, the experimental findings reported by Roshko leave a clear possibility that periodic vortex shedding may be encountered at the high flow Reynolds Number associated with Saturn V ground wind conditions. In any case, sufficient substantiation of periodic vortex shedding for Saturn V/Apollo ground wind conditions has been found to merit serious consideration of its implications.

The existence of periodic vortex shedding at any Reynolds Number above subcritical is a radical alteration of fluid flow concepts that have been accepted for many years. Further substantiation of this phenomenon in its simplest form is believed necessary. Dr. Y. C. Fung, in a recent informal conversation, pointed out that the wake periodicity observed by Roshko is not incontrovertible evidence of similarly fluctuating aerodynamic forces on the cylinder. He implies that this periodicity may be developed within the wake itself.

If periodic vortex shedding from a cylinder exists at higher Reynolds Numbers, the inability of current wind tunnel facilities to reproduce full-scale Reynolds Numbers will become a serious limitation to test results,

particularly if "fixes" such as spoilers, windscreens, splitter plates, and other flow alteration devices are to be investigated. Although a particular device may be found satisfactory at maximum test Reynolds Numbers, which are on the order of 6 to 7 million, its satisfactory operation at full-scale design Reynolds Numbers of 15 to 20 million and under natural conditions is not assured.

Finally, it may be stated that current ground wind loads criteria, which do not allow for periodic vortex shedding, produce critical loads on the S-II stage. Stringer spacing of the hydrogen tank wall is set by ground wind conditions. Launch release during a design wind produces loads on the Apollo structure which are close to critical. Added consideration of periodic vortex shedding for structural design would in all probability result in a structural weight increase.

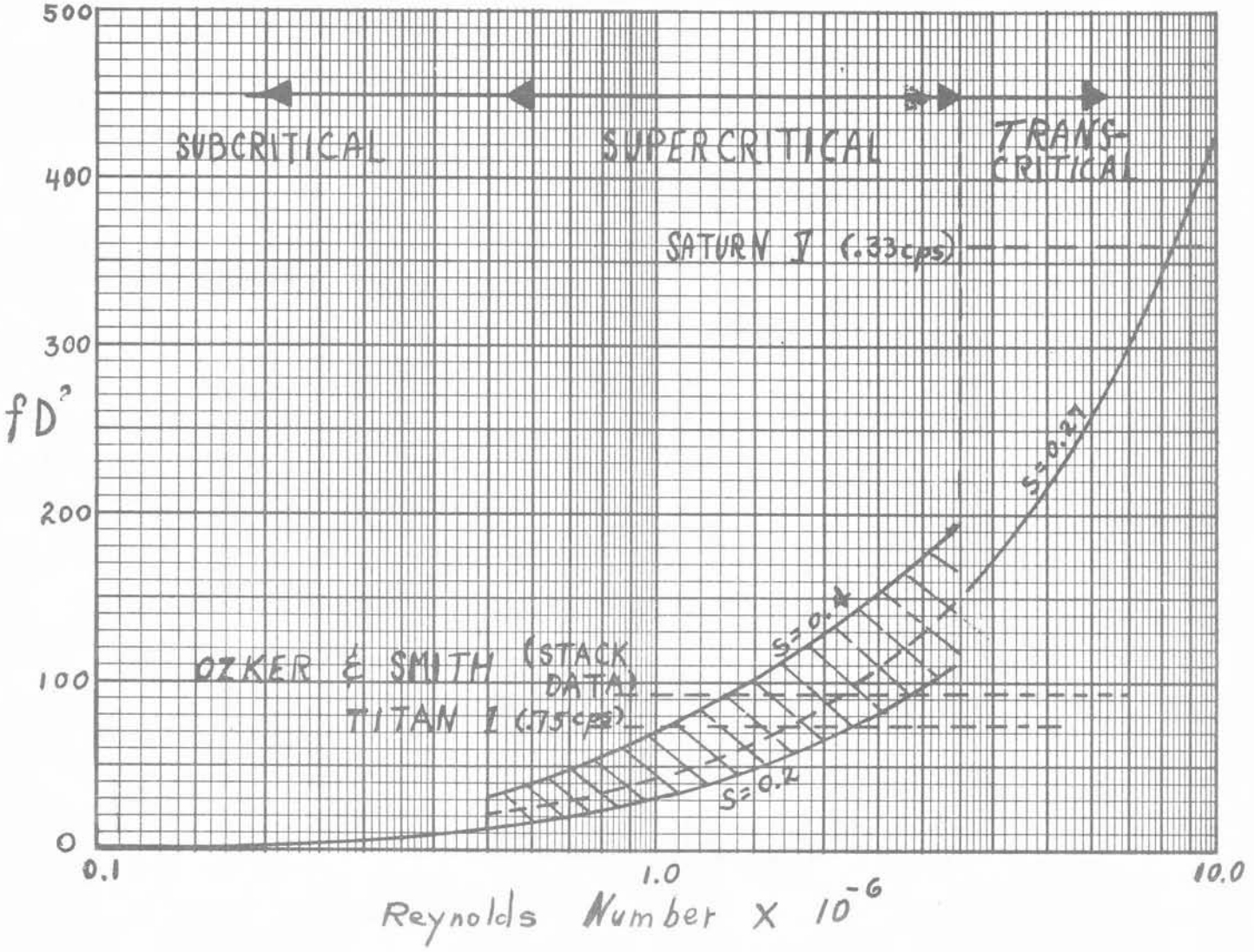

Figure 3. Full-Scale Frequency Comparison

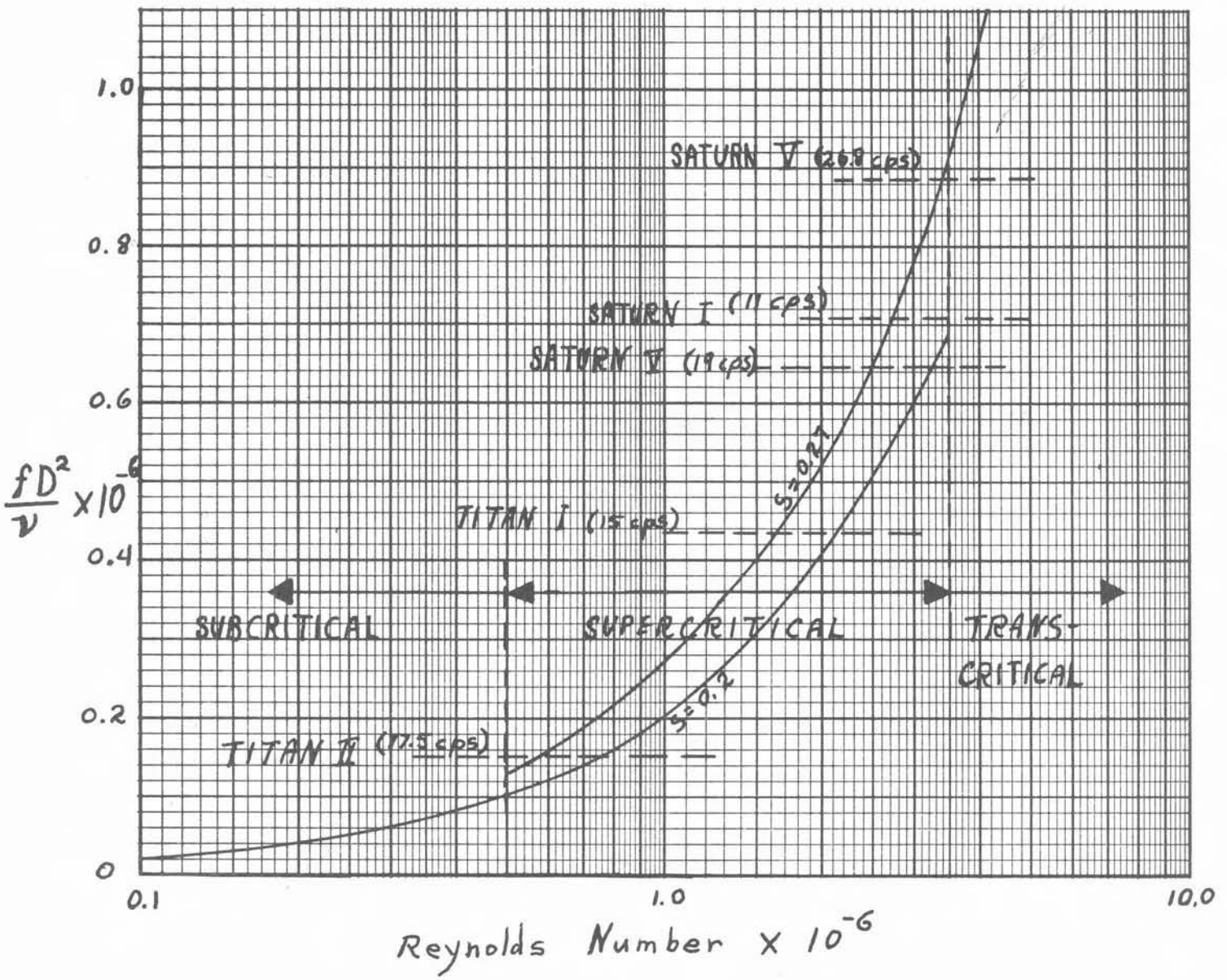

Figure 4. Frequency Comparison of Various Test Models

3. Acoustic Environment at Launch

During the launch phase, two major sources of noise are important: rocket engine noise and aerodynamic noise. Both have a random character and a broad frequency spectrum. Rocket engine noise predominates in the brief subsonic part of the launch, after which aerodynamic noise prevails. The rocket noise is generated in the exhaust stream and transmitted through the air to the vehicle surfaces. At lift-off, it is also reflected from the ground surface. The noise level is a function of engine power and the distance from the booster aft end to the payload region. Maximum overall sound pressure level (SPL) of this noise at the payload end is expected to be in the 140 to 150 db. range. Figure 5 shows the general pattern of the noise time history.

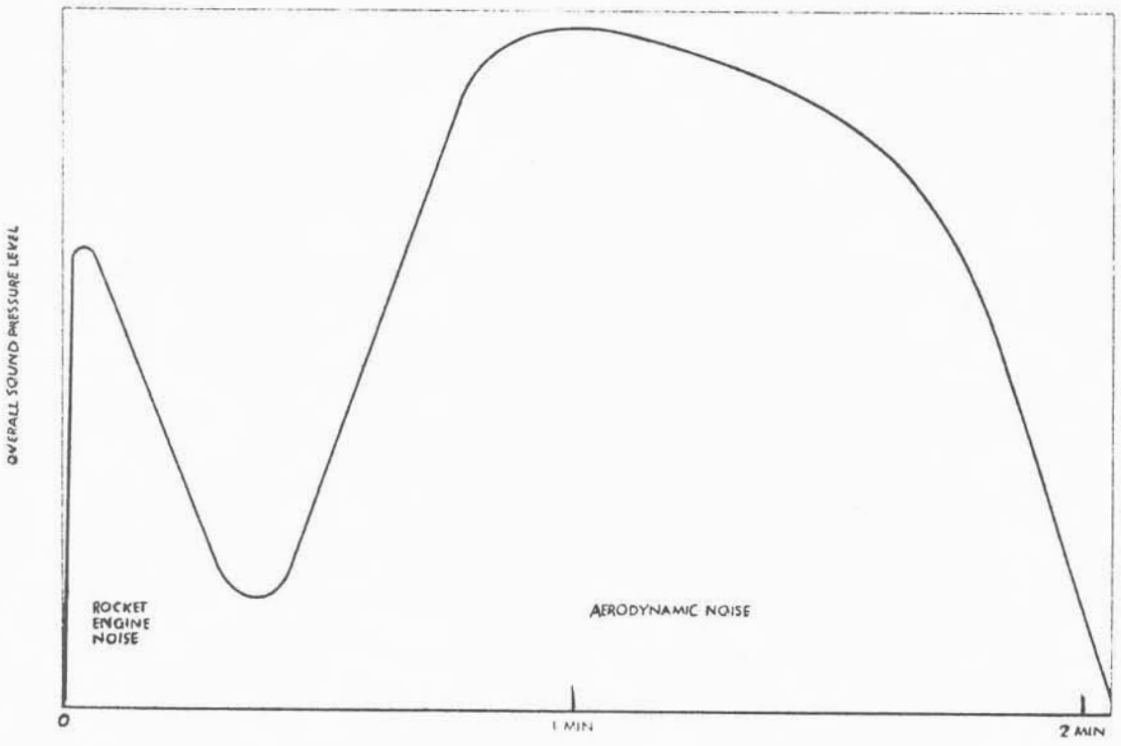

Figure 5. Time History of Overall External Acoustic Levels

4. Vehicle Response to Acoustic Environment

The topic of response of a difficult-to-define structural system to acoustic excitation is receiving some attention these days and hopefully will be researched more thoroughly in the future.

Present practice seems to be to review as much data on similar systems as possible and to relate the measured vibration levels of the known system to its acoustic field. Then by predicting the acoustic level of the new design, an estimate of the vibration response of the new system is made. While this seems to be an effective engineering approach, refinements and improvements are desired. The source of vibration and acoustic noise in a typical missile are shown in Figure 6.

It is important to note here that ground equipment, vehicle equipment, and often payload equipment must operate in this vibration environment induced by the acoustic environment.

A word of caution to you structural dynamists -- don't make the mistake of overlooking the bracket, or means of attachment, between functional components and basic structure. Many of us have discovered the hard way that inadequate mounts can show up in a system design.

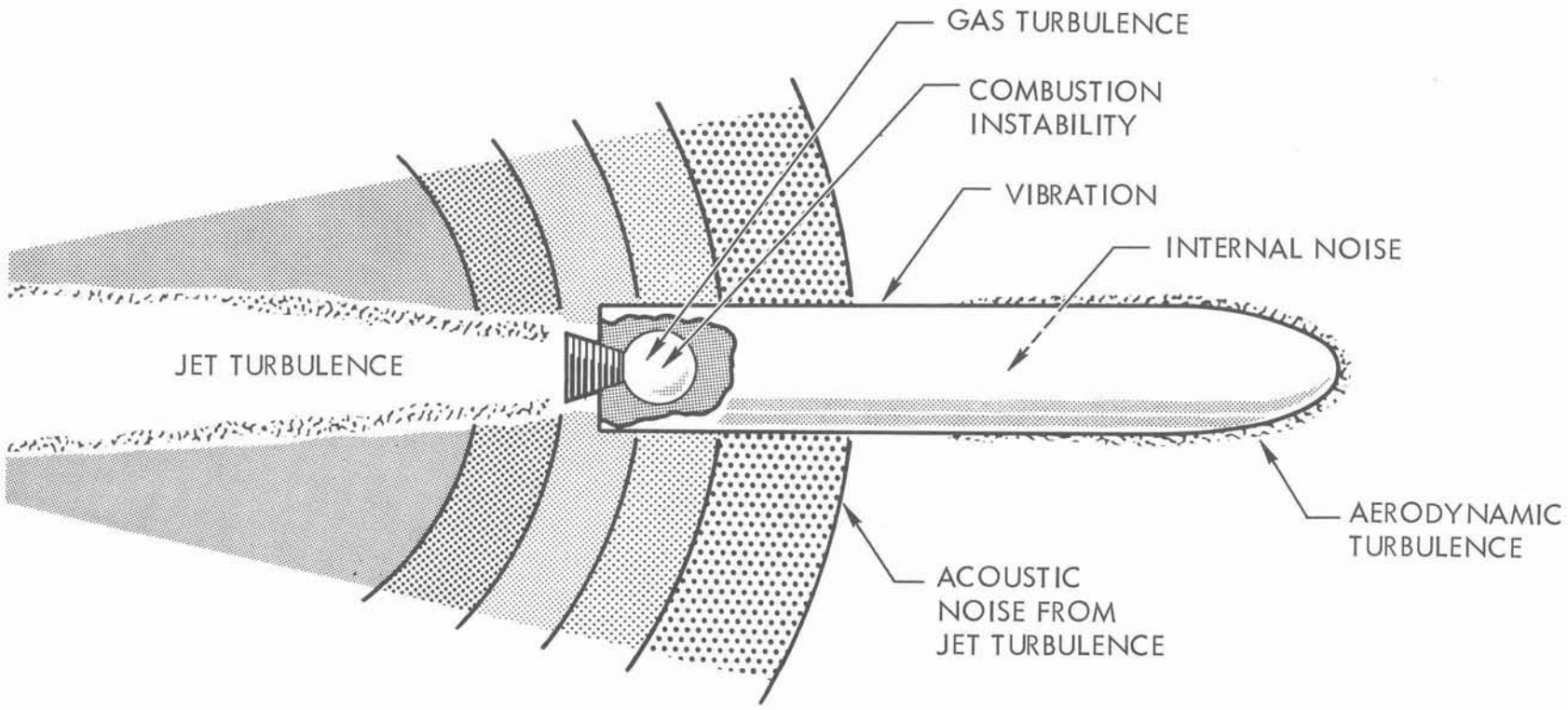

FIGURE 6. SOURCES OF ACOUSTIC VIBRATION

5. Thrust Buildup Structural Transient

The ignition of a modern rocket engine applies large loads rapidly and somewhat randomly with respect both to time of starting the buildup and the slope of the buildup curve. Since the engine is the forcing function and it has variations, a statistical model for the forcing function must be established.

Now when multiple engines are contemplated in design, there may be some beneficial structural dynamic effects from staggering the engines. Here the idea is to oppose the first dynamic transient with the proper phasing of the second transient.

Another way to reduce the dynamic load factor would be to decrease the rate of thrust buildup.

In Chapter 3 of Structural Design for Dynamic Load, (McGraw Hill, Norris et al.) the structural response of a one-degree-of-freedom system is discussed and the dynamic load factor is presented for some discrete types of time-varying load applications.

Higher longitudinal modes should be considered to assure that excessive loading is not imposed on the system. Lateral modes should be considered for unsymmetric loading produced by the randomness between symmetric engines. This effect could penalize certain types of payloads as well as other types of structure and equipment.

In design analysis this effect should be considered in combination with the wind oscillatory and steady-state effects. Figures 7 and 8 show typical thrust buildup structural transients, and shear and bending-moment distribution at launch, for a space vehicle of the Saturn V configuration.

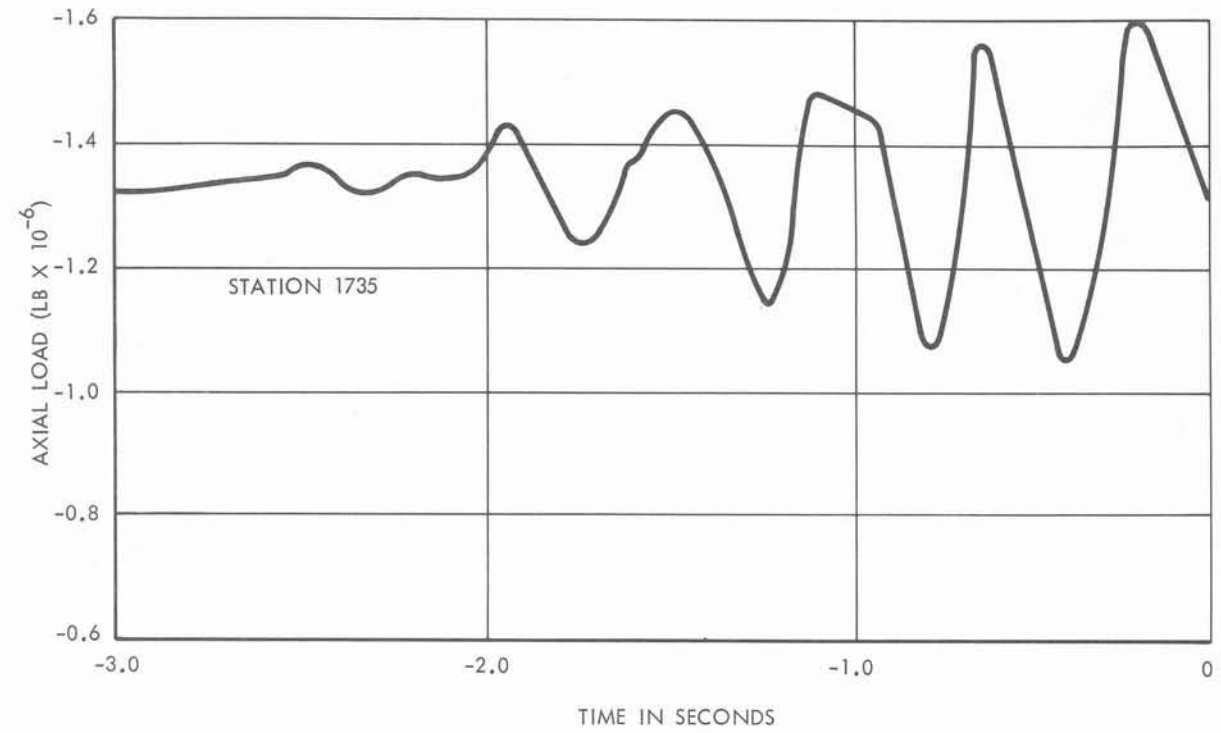

NOTE: ALL VALUES ARE LIMIT

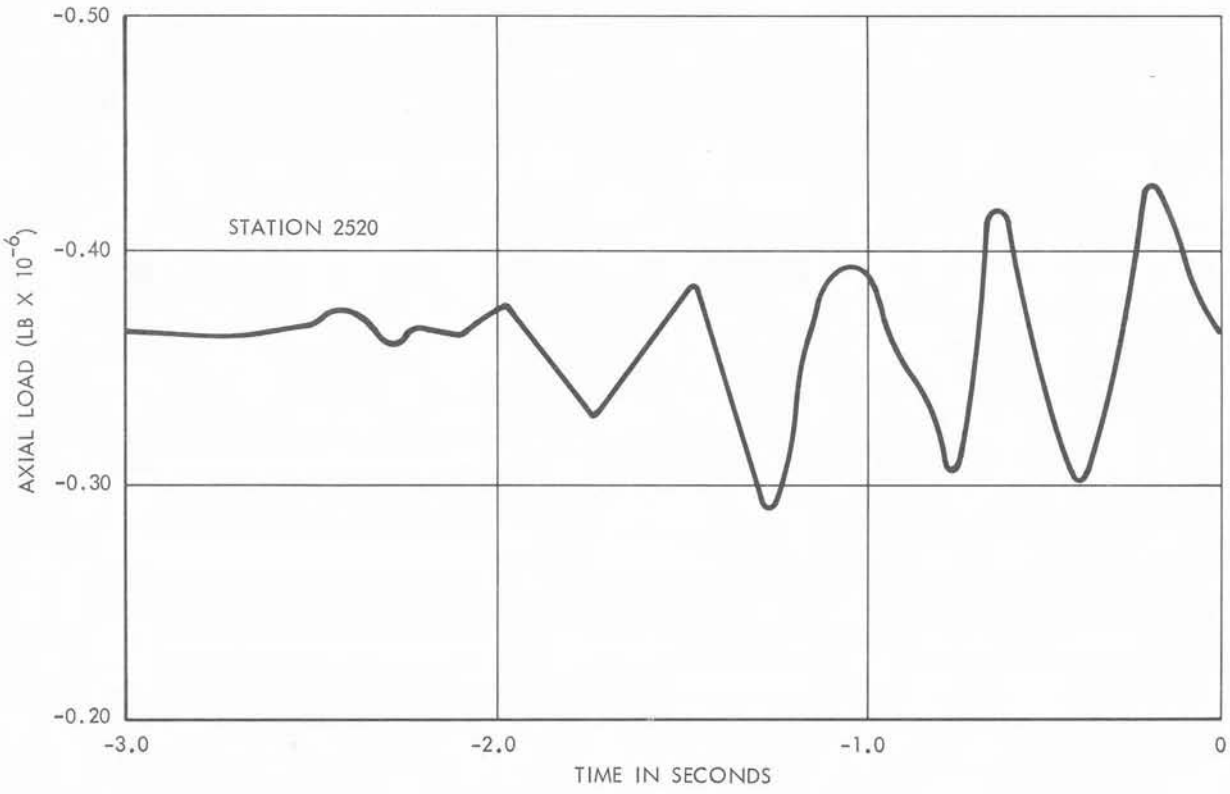

FIGURE 7. THRUST BUILDUP STRUCTURAL TRANSIENT

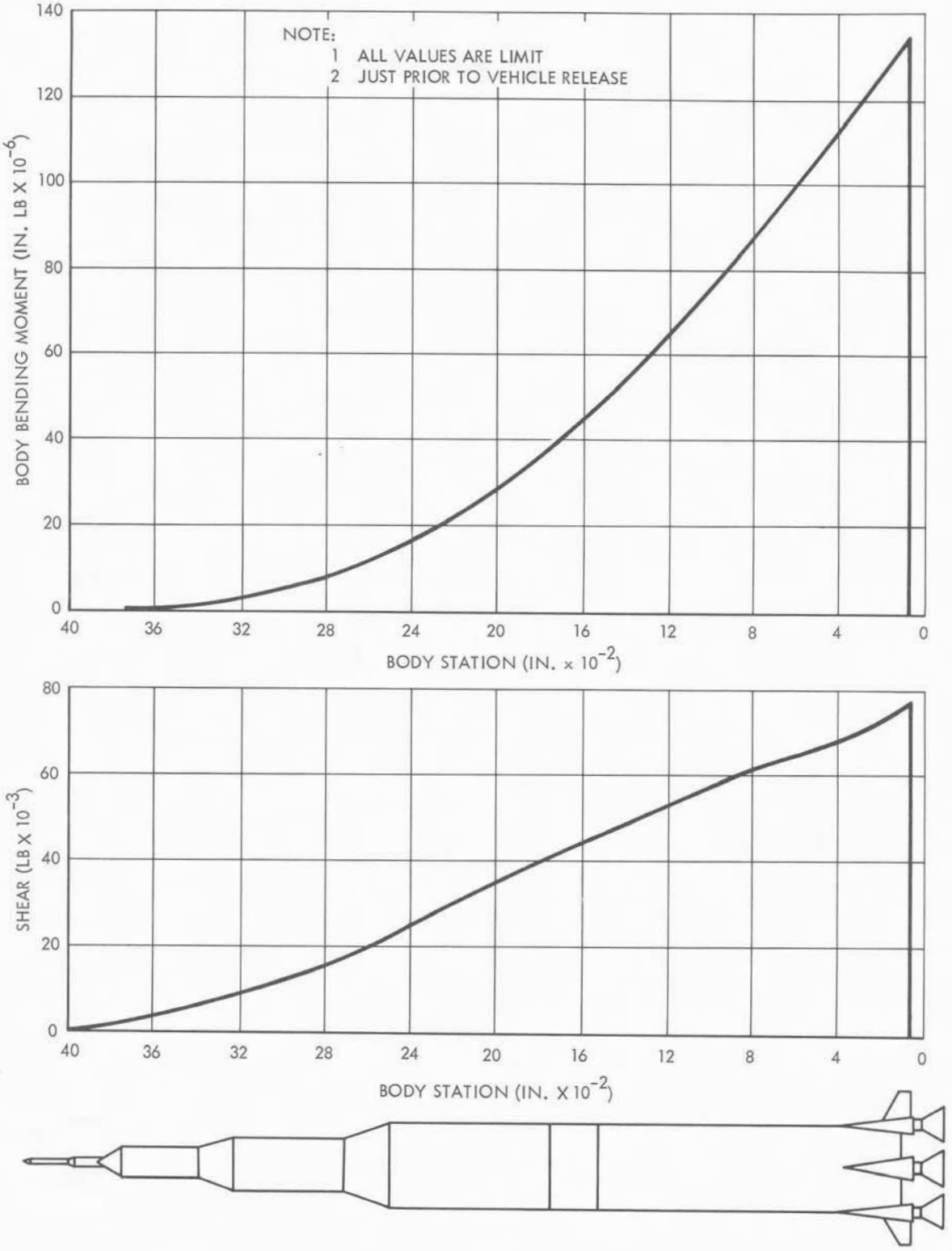

FIGURE 8. SHEAR AND BENDING-MOMENT DISTRIBUTION AT LAUNCH

6. On-Pad Abort Structural Transient

The on-pad abort structural transient is the same basic phenomenon as the previously mentioned thrust-buildup transient. Here it is the removal of large forces rather rapidly when the engines are shut down.

In general, the thrust decay curve has a lower average negative slope than does the thrust buildup curve have a positive slope and, in addition, is usually more repeatable or, if you prefer, has a smaller standard deviation.

There are some combined loadings that should be considered here:

1. the thrust buildup dynamic load factor,
2. wind influence, or
3. an engine failing to start

may be the reason for the abort. These may combine in various ways and some statistical approach is probably very much in order.

Again some reduction in loads may result from sequencing the shutdown time between symmetric groups of engines.

Figures 9 and 10 are examples of the on-pad abort structural transient at two selected stations, and axial load distribution at rebound.

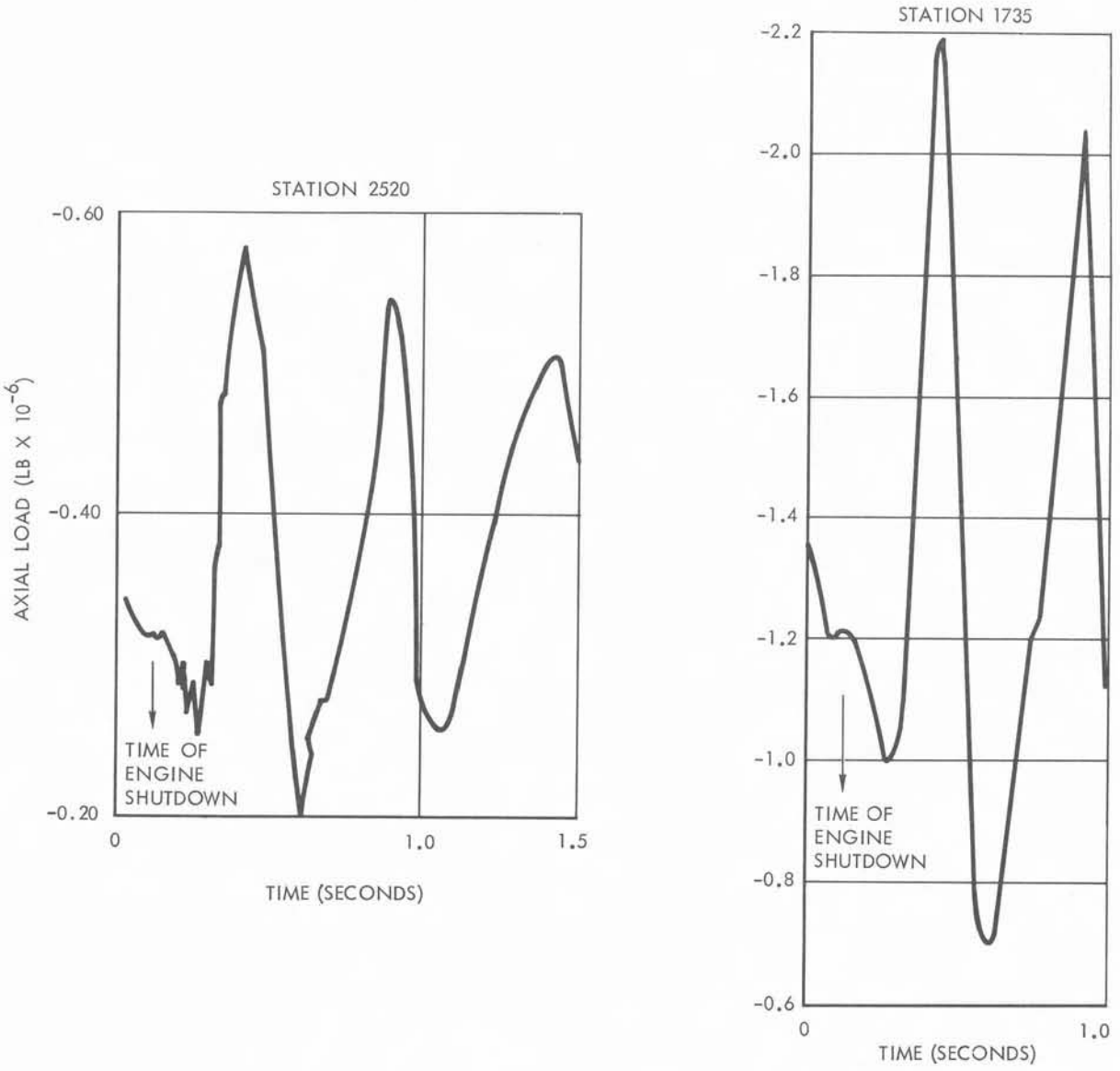

FIGURE 9. ON-PAD ABORT STRUCTURAL TRANSIENT

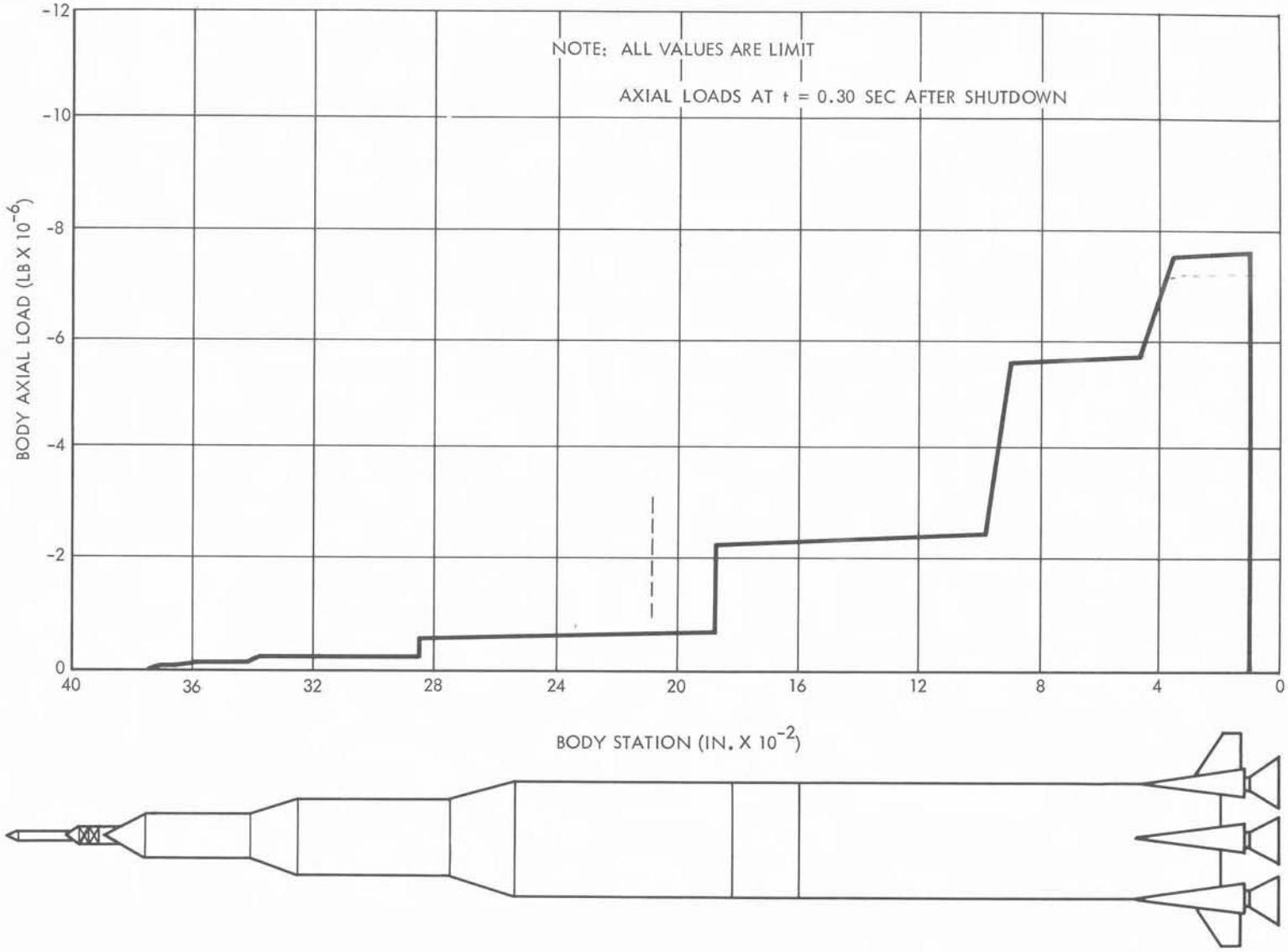

FIGURE 10. AXIAL LOAD DISTRIBUTION AT REBOUND

7. Launch Release Structural Transient

The sudden release of a vehicle tied to the launch pad, with loads applied as ground winds and gusts, results in oscillations of the vehicle due to the excitation of the free-free modes. (Refer to Figure 8.) The initial conditions depend on the prelaunch loads history with essentially a negative step input of the tie-down reactions at time zero. An example of the structural transient at launch release is shown in Figure 11. The time history of the bending moments and shears at any vehicle station consists of the summation of sinusoidal damped oscillations of all modes required to adequately represent the dynamic response, together with the portion of the steady state response which may be statically calculated. (See Figure 12.) This condition is critical for the upper stages of the vehicle where the static loads prior to launch are magnified by a large factor.

The longitudinal dynamic load calculation is similar to the lateral condition using axial modes. Consideration must be given to the engine starting sequences and the time history of thrust together with launch pad flexibility and time of release.

Besides influencing the structural design of the system, this sudden release could trigger the "pogo" problem if that instability existed for the system at that time. Axial load distribution at time of release for a vehicle of the Saturn V configuration is shown in Figure 13.

Such connections along the side of the vehicle as egress arms, propellant topping lines, and umbilical arms produce kick loads upon their release at lift-off which should be looked into with regard to vehicle-payload problems and also with regard to ground equipment problems.

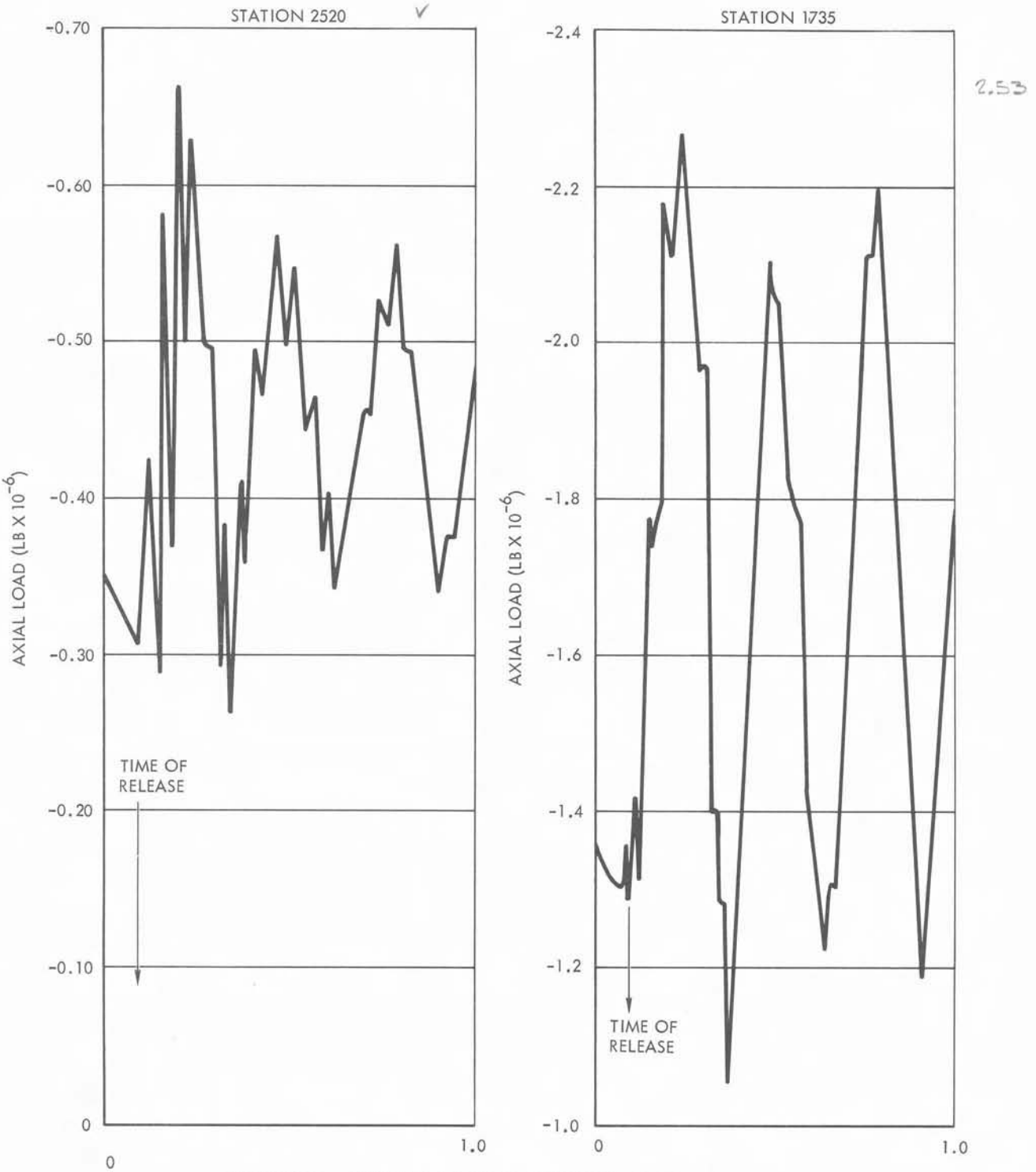

FIGURE 11. LAUNCH RELEASE STRUCTURAL TRANSIENT

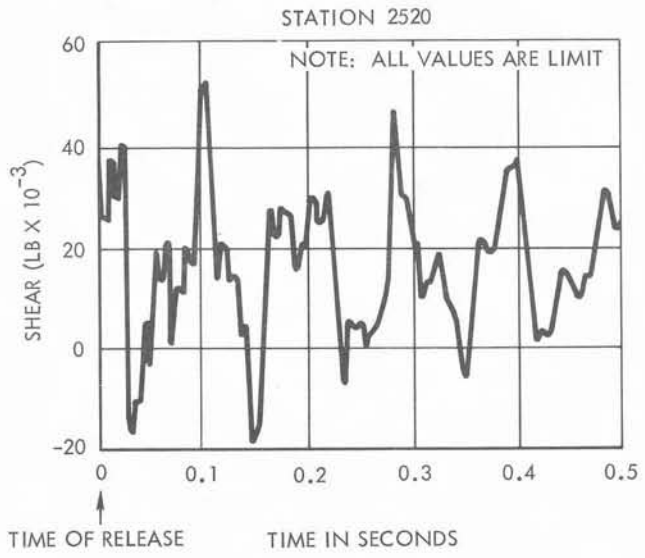

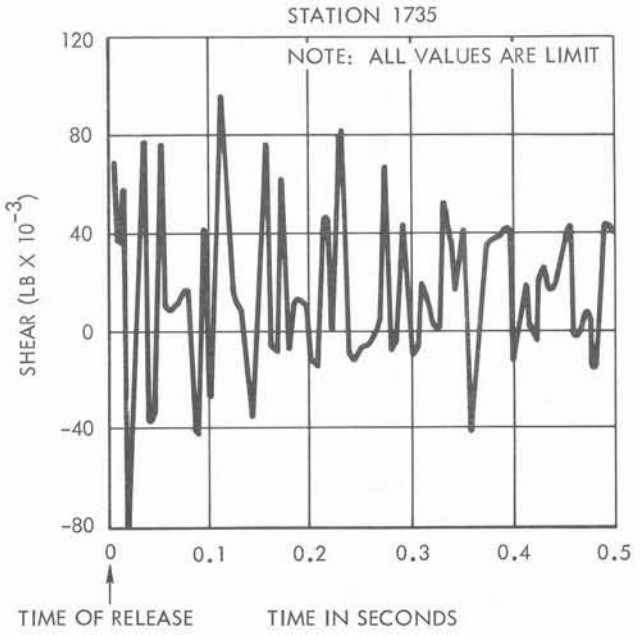

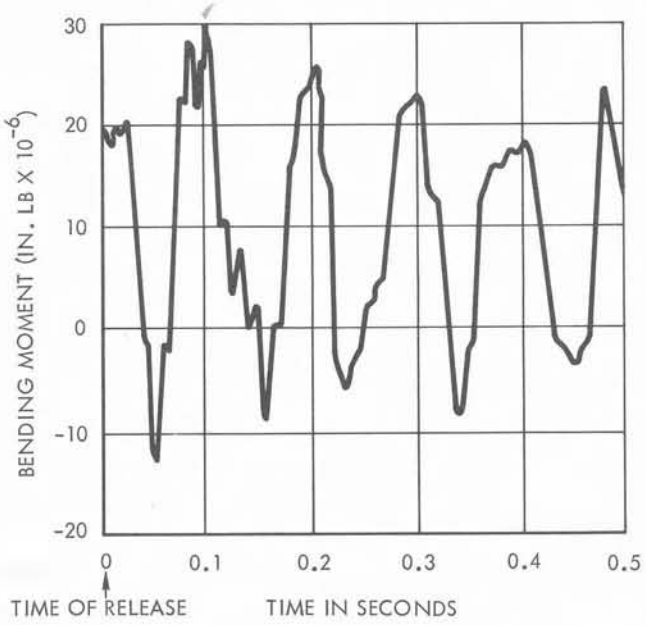

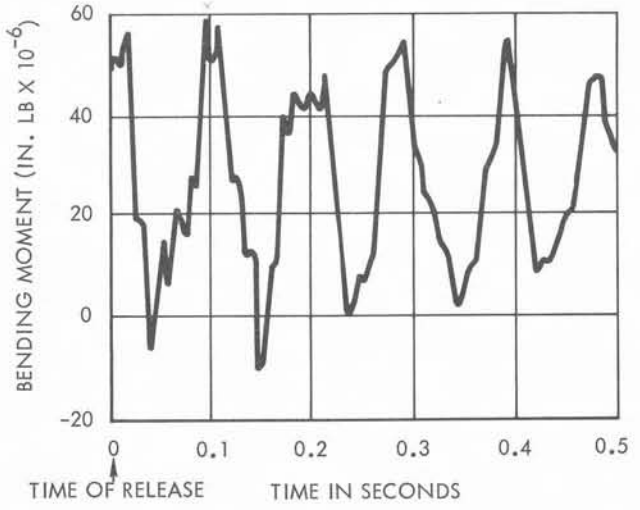

FIGURE 12. SHEAR AND BENDING MOMENT HISTORY AT RELEASE

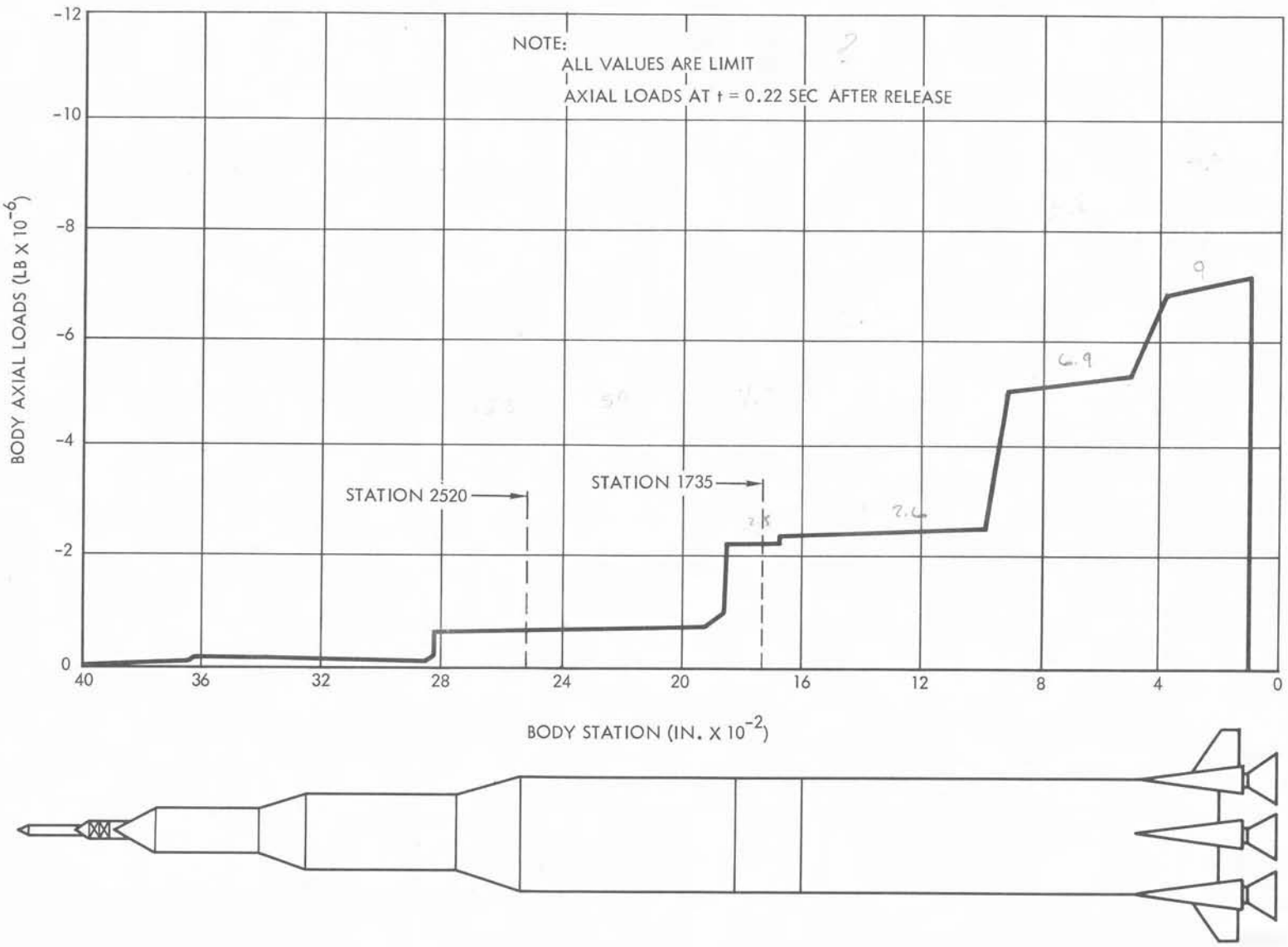

FIGURE 13. AXIAL LOAD DISTRIBUTION AT RELEASE

8. Acoustic and Buffeting Environment in Flight

The problems associated with successful operation of launch vehicles in their acoustic environment have multiplied in recent years. Booster engine thrust has increased rapidly without a parallel increase in vehicle surface density and stiffness. Mission requirements have often dictated the use of composite vehicles with a resulting compromise in aerodynamic performance. As stated earlier, the acoustic environment is due primarily to two sources: booster engine noise and aerodynamic noise. At high velocity flight through the atmosphere, aerodynamic noise from the turbulent boundary layer is the more significant.

Booster engine noise is a by-product of turbulent mixing of the exhaust gases with the surrounding air. The effective acoustical sources are distributed along the jet exhaust, with the high frequencies generated close to the nozzle. The most intense noise is generated in the subsonic portion of the exhaust flow. During subsonic flight, engine noise will be propagated through the atmosphere to the vehicle skin, resulting in mechanical vibratory response.

Empirical methods have been developed to determine the overall acoustic power and spectral distribution of acoustic energy generated by the booster engines. These methods have proved adequate for preliminary analyses of proposed launch vehicle systems.

However, it is recognized that the assumptions used in these studies are no longer valid in the near and intermediate field of large booster vehicles. In the near field of these acoustic sources pressure and velocity of the disturbance are not everywhere in phase, making the determination of

energy in the near field difficult. The extremely large fluctuations in the near field cause nonlinear propagation effects which have not yet been fully explained.

Since booster engine noise is produced by turbulent mixing of the exhaust stream and must be propagated forward to the vehicle skin, it will not be observed on the vehicle at supersonic speeds. Noise from aerodynamic sources will begin to predominate during transonic flight. A variety of aerodynamic sources may contribute to the composite environment. Most of these sources will be pseudo-acoustic in nature. Sonic-induced vibration of the structure will occur as a result of the transfer of momentum by impingement of turbulent eddies on the vehicle skin. These eddies will form as the result of viscous interaction between the vehicle skin and the surrounding air, or turbulent flow separation caused by abrupt changes in vehicle geometry.

Preliminary studies have indicated that the flow disturbance caused by protuberances on the vehicle surface will cause an acoustic environment much more severe than that resulting from the customary attached turbulent boundary layer. At transonic speeds, a weak normal shock wave is formed forward of the protuberance, and under the proper conditions of Reynolds number and Mach number the interaction of this shock wave with the boundary layer will be unstable, causing longitudinal oscillation of the shock wave resulting in large-scale, low-frequency pressure fluctuations on the vehicle skin. This phenomenon is thought to be the triggering mechanism for transonic buffet and has been observed near body discontinuities and abrupt changes in flow deflection angle. Another source of intense noise in the forebody

region of the protuberance will be caused by convection of turbulence through the shock wave. This phenomenon has been recognized as the mechanism involved in the screech of choked jets, but verification is required to justify the analogy with the present case. Although this energy will be primarily radiated forward of the protuberance, there will also be a contribution to the afterbody acoustic environment.

The afterbody noise is due primarily to eddies shed by the projection. At low Reynolds numbers, a regular pattern of eddies is shed from the projection giving rise to the classical Aeolian tone. As the Reynolds number increases, three dimensional effects are observed, the flow becomes turbulent and in contrast to the discrete energy of the Aeolian tone, the acoustic environment becomes random and is best described by a power spectrum. The classical Aeolian tone has been well described by a number of researchers using Lighthill's theory of sound generated aerodynamically. However, a combined analytical and experimental study is required to extend the theory to transonic and supersonic flow.

This study should include the effect of projection shape and size on the intensity and spectral distribution of energy in the wake. Further research is also needed to develop a theory for the oscillating shock wave turbulent boundary layer interaction and to verify the scaling laws used for estimating the aerodynamic noise of flight vehicles based on data from wind tunnel tests of scale models. These scaling laws are questionable because of the large dimensional ratio of the model to the full-scale vehicle and the necessity for compromising some flow parameters during wind tunnel testing.

9.0 Coupling of Engine and Vehicle Dynamics

It is known from past experience in launch vehicle systems that the interaction of the propulsion system and the longitudinal modes of the vehicle may cause chugging of the engine. The system interaction is most easily shown by the closed loop schematic diagram in Figure 14. The thrust of a given engine depends primarily on the propellant flow rate and the mixture ratio. The thrust acts on the vehicle, excites the longitudinal modes which in turn cause pressure fluctuations at the bottom of the fuel tanks. The resulting fluctuations in the pump inlet pressure result in a variable flow rate through the feed lines. This may cause bubble formation at the pump inlets for cryogenic fuels which have high vapor pressures and require high flow rates. The bubbles would cause the propellant to act as a compressible fluid and would have the effect of adding a pneumatic spring to the system. In a typical case, the pump discharge pressure depends on the inlet pressure and the pump speed. The propellant is tapped from the pump discharge line for use in the gas generator. The gas generator is used to power the turbines which drive the propellant pumps, thus completing the cycle.

In order to properly analyze the complete system dynamics, the complete transfer function for the engine system is required. This information, however, is not available from engine manufacturers and an advance in the "state-of-the-art" is required. At present, one can only obtain those influence coefficients which are based on steady state conditions. The use of these coefficients cannot reflect any phase lag which occurs in the system and is analogous to using the constant stability derivatives (C_{l_α}) in flight dynamics.

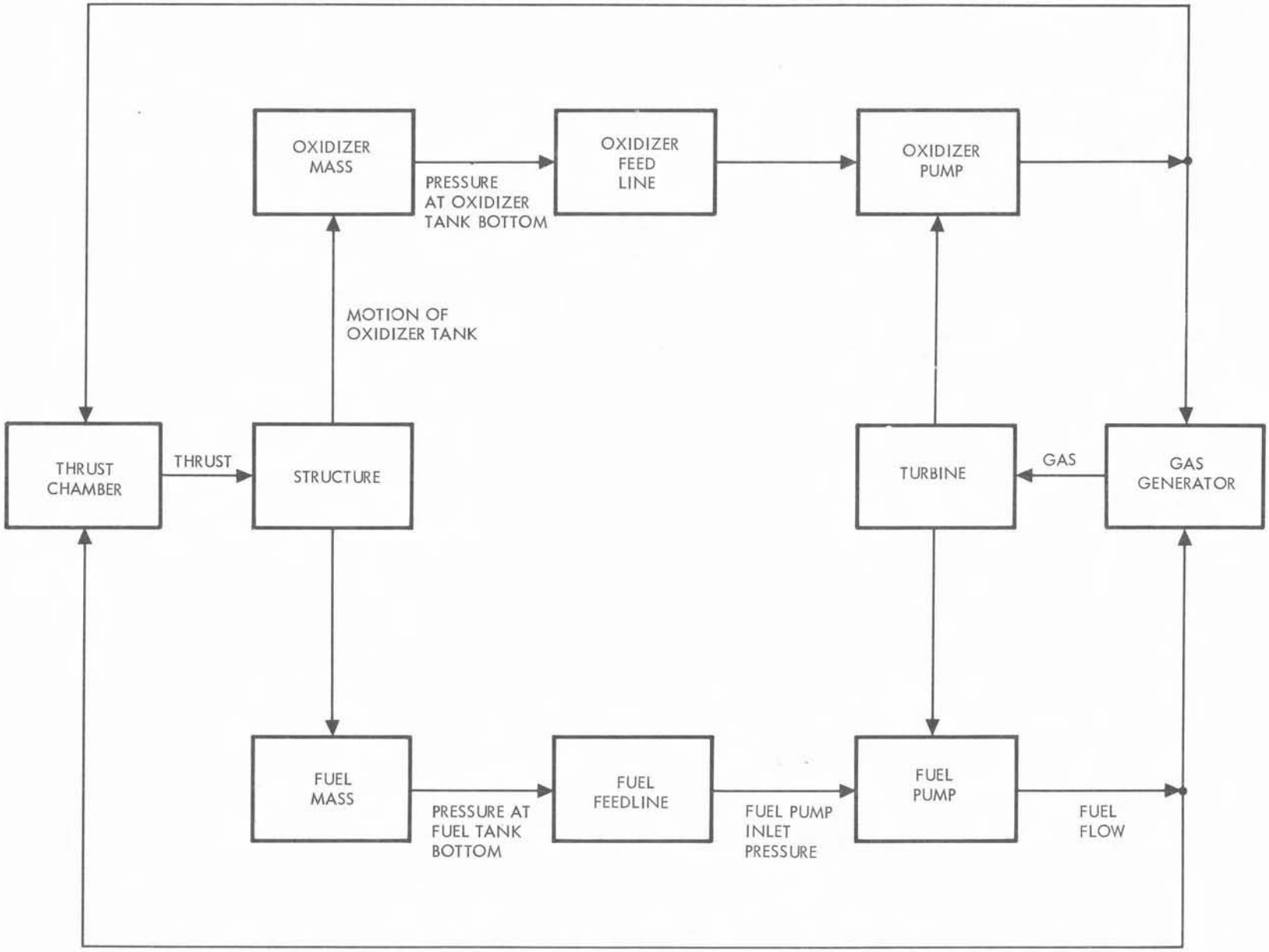

FIGURE 14. COUPLING OF ENGINE AND VEHICLE DYNAMICS

9.1 Longitudinal Vibration Modes

In order to improve the method of obtaining longitudinal vibration modes a more sophisticated approach is required in analyzing the behavior of the propellant in the bulkheads of space vehicles. The bulkhead of a launch vehicle may be idealized as an oblate spheroidal tank partially filled with an inviscid incompressible fluid. The natural frequency of this system involves the interaction of the fluid and the spheroidal shell at their interface.

The mathematical formulation of the shell equations are most easily done by use of oblate spheroidal coordinates. This coordinate system is also convenient for specifying the compatibility of the fluid and shell velocity normal to their common surface. Difficulty, however, is encountered in specifying the pressure at the free liquid surface. It therefore seems advisable to first solve the problem of a completely filled spheroidal tank and thus avoid this difficulty. An effective mass density could be used to produce the same total weight. It is reasonable to assume that for nearly full tanks the above assumption is valid.

A Rayleigh-Ritz approach to this problem, in which one assumes the mode shapes for the liquid-filled shell, has been successfully applied to cylindrical shells. The natural frequency of the axi-symmetric vibrations of an empty prolate spheroidal shell has also been obtained. The modes may be similarly obtained for an oblate spheroid and may be used in a simplified form for the assumed modes.

The determination of the mode shapes and frequencies for a bulkhead with a free-liquid surface will require the development of new techniques.

9.2 Propellant Line Dynamics

The vibration of a tube with internal flowing fluid has been studied by G. W. Housner, R. H. Long, and F. Niordson. Housner and Long assume the tube to act as an Euler beam in flexure and Niordson develops the more general case in which the tube is treated as a shell. Some results are available for the former case in terms of series solutions. From the results obtained thus far for the beam, it appears that at a certain critical velocity the natural frequency of the system is reduced to zero and a propellant line reacts very much like a beam column and is unstable. Niordson's formulation of the problem is quite thorough but he is unable to solve the shell equations except for the case in which the velocity of the flowing fluid is zero.

Considerable work needs to be done before the dynamics of propellant lines can be properly understood. The available approximate solutions for even the beam equations cannot be considered as the final results to this problem. The effects of fluid viscosity and the turbulent boundary layer on the oscillations of the tube are unknown and require investigation.

10. Vapor-Liquid and Bulkhead Interaction During Engine Cutoff Transient

The abrupt removal of the thrust load at the end of a boost stage may produce a transient liquid-shell response at the vehicle bulkhead. (See Figure 15.) This response arises from the sudden release of strain energy stored in the bulkhead during the boost phase, which must be converted to kinetic energy by the enclosed liquid fuel. Because of the nonlinear time-dependent boundary conditions at the free surface, this problem is not easily solved.

The vibration of shell structures with and without internal fluids has been determined by a number of investigations. These methods assume an appropriate trigonometric series for the mode shapes and obtain good results for shells of uniform thickness. The problem of reinforced shells, however, does not lend itself readily to this method of attack and a more practical engineering approach is required. With the presence of bulkheads and contained fluids, the dynamic response of shells to periodic and random oscillations is extremely hard to analyze.

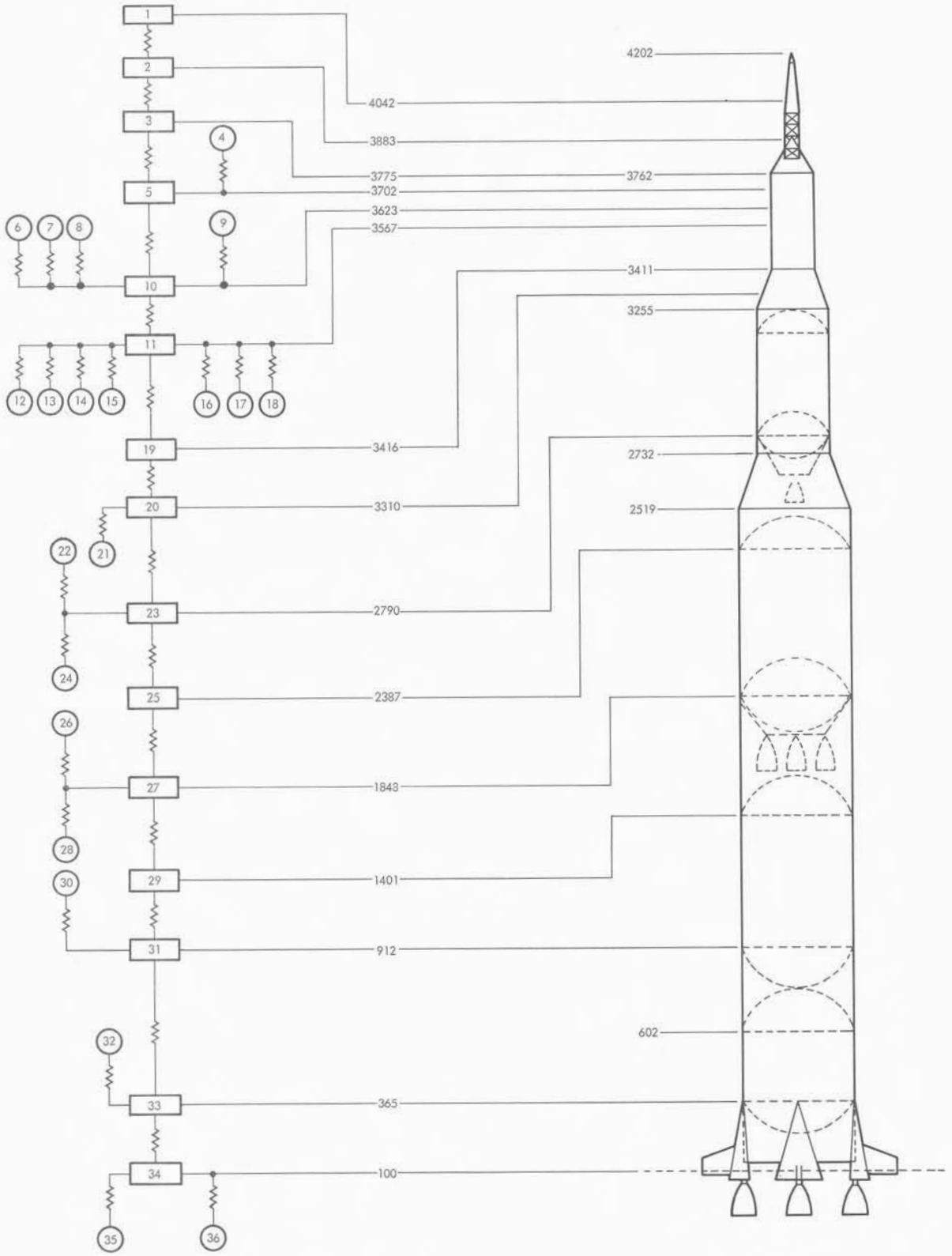

FIGURE 15. SPRING-MASS REPRESENTATION OF THE SATURN V VEHICLE

11. Separation of Stages or Shrouds (Jettisoning)

The primary loads occurring during staging are due to engine thrust cut-off and starting transients. The sequence of engine thrust cut-off for the spent stage and engine start for the succeeding stage represent the forcing function for these load conditions. In the loads calculation, the transition from pre-separation to post-separation vehicle dynamic systems is accomplished by determining the boundary conditions at the time of separation. A proper design requires a compromise between a coast period long enough to permit shutdown of the engines of the preceding stage, but not so long as to impair attitude control capability. Detailed studies of the separation sequence are vital to optimize design.

12. Dynamics of Fluids under Low-g Environment

Some work has been done for simple geometric problems of oscillation of liquid-vapor interface about equilibrium configurations. (See Figure 16.) Infinitesimal oscillations of a globule of liquid and a vapor bubble caused only by the action of surface tension forces may be found in Lamb. Free surfaces of equilibrium configurations in low-g environment may be expressed only in terms of series expansions. Natural frequencies and their mode shapes can be obtained once the appropriate Green's function is determined. Because of the complexity of the free surface boundary conditions, the only known method for solution is the use of appropriate numerical procedures.

Transient response of a liquid in a zero or low-g environment is another area in need of study. Computer programs must be developed to provide solutions for variable boundary values.

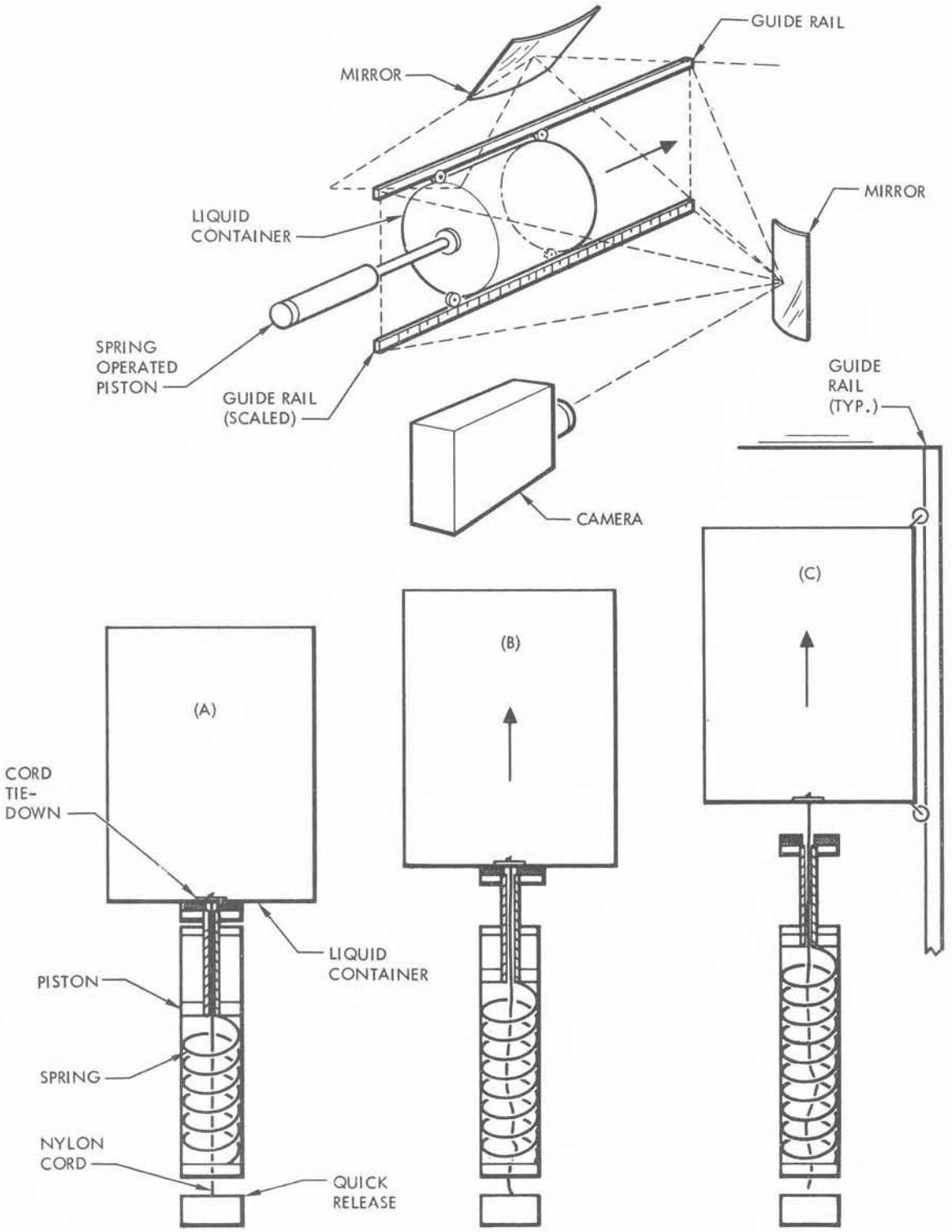

Figure 16. Test Configuration for Determining Liquid Response to Tank Rotation

13. Rendezvous and Docking

Docking loads originate during the interval of time from first physical contact or connection to final vehicle latching. The pre-contact or pre-connection thrusting is considered as part of the rendezvous maneuver. Docking impact is shown in simplified form in Figure 17. The load magnitudes introduced during docking are primarily a function of (1) initial conditions relating vehicle alignment and relative velocity; (2) physical data describing vehicle mass, mass moment of inertia and CG locations; and (3) arrangement and flexibility of the docking mechanism members and immediate backup structure. A number of docking mechanisms have been and are being investigated for the Apollo-IEM docking studies. Much work must still be done to develop docking design criteria and methods for analysis of space station docking loads.

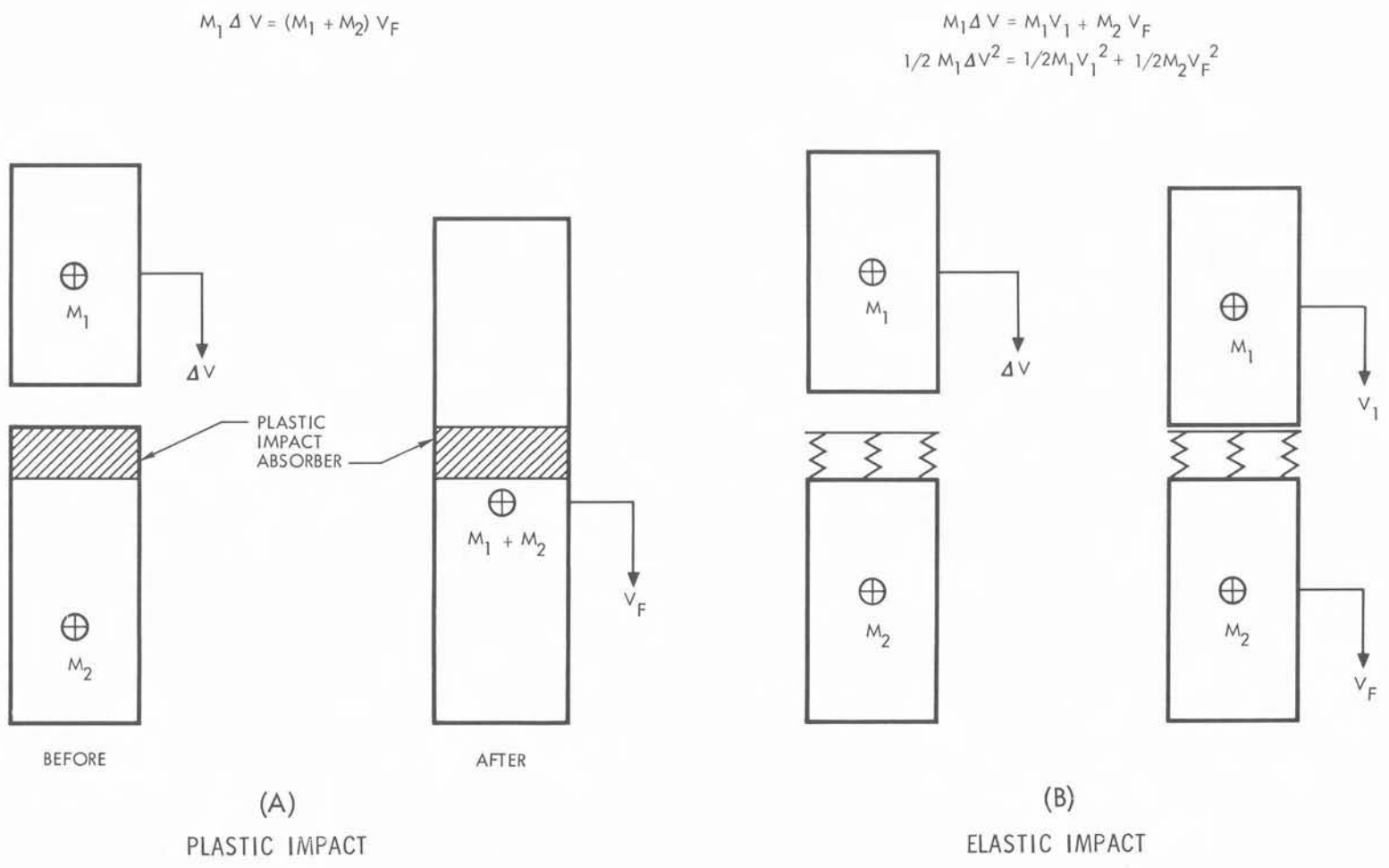

Figure 17. Simplified Presentation of Docking Impact

14. Stabilization of Space Stations with Cable-Connected Configurations

Analysis of the transient response of the spinning compartment-cable-counterweight space station has shown that large wobble angles will result from slight disturbances. However, analysis of the response to gravity gradients is inconclusive.

The free vibrations of the compartment-cable-counterweight space station were analyzed by a method based on the classical linearized approach. The lateral vibration of the configuration was carried out by both the lumped parameter method and continuous representation in the form of partial differential equations. The results obtained from the two methods are consistent. The lateral vibration with the angular rotation of end masses was also studied. The effect of end rotations do not significantly change the mode shape except at the end near the counterweight in the first and second mode; the frequencies are higher than those without end rotation. The increase in frequency ranges from seven percent in the fundamental mode monotonically decreasing to one percent in the fifth mode. (See Figure 18.)

The stability analysis of the compartment-cable-counterweight configuration (see Figure 19) reveals that in order to keep a real and positive nutation angle α, the magnitude of energy dissipation $\Delta T/T_e$ is restricted by the ratio of the maximum moment of inertia I_x to the intermediate moment of inertia I_y. The smaller the ratio $\frac{I_x}{I_y}$, the more sensitive is the stability of the configuration to the amount of energy dissipation. Since $\frac{I_x}{I_y} = 1.00874$ for the cable configuration, the maximum possible value of $\Delta T/T_e$ is around 0.001. For $\Delta T/T_e = 0.001$, the nutation angle α varies between α min = 0.0934 degrees and α max = 19.775 degrees.

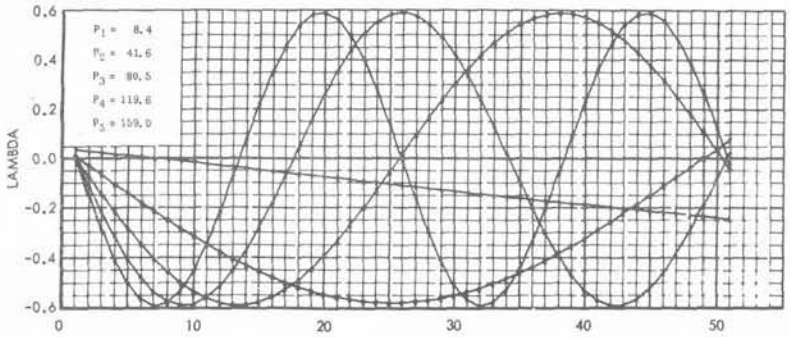

(A) LONGITUDINAL VIBRATION - NORMAL MODE

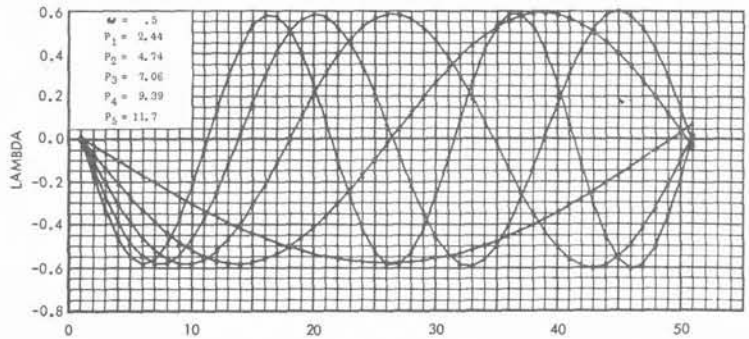

(C) TORSIONAL VIBRATION - NORMAL MODE

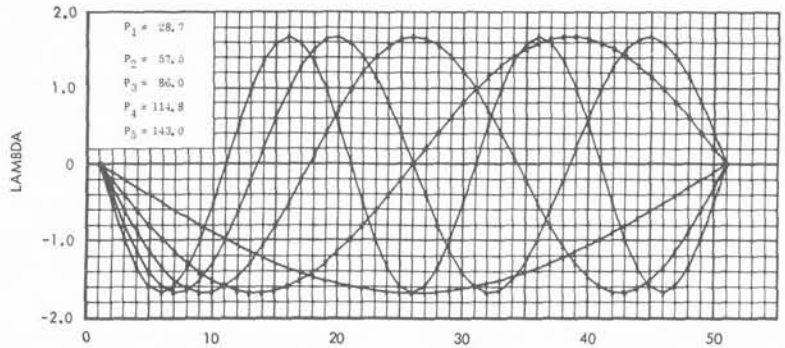

(B) LATERAL VIBRATION - NORMAL MODE

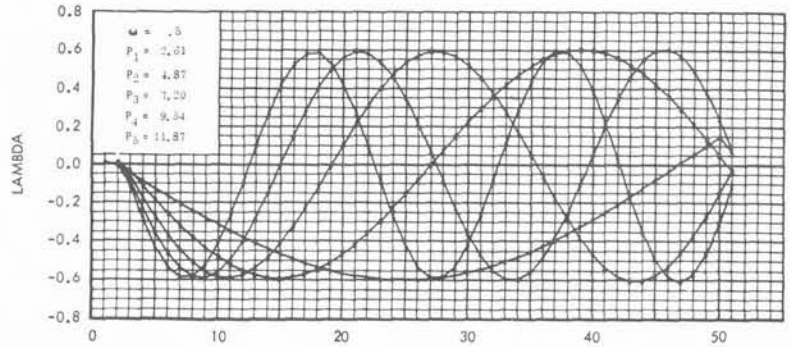

(D) LATERAL VIBRATION WITH ROTARY INERTIA OF COMPARTMENT AND COUNTERWEIGHT - NORMAL MODE

Figure 18. Vibration Modes of Cable-Connected Space Stations

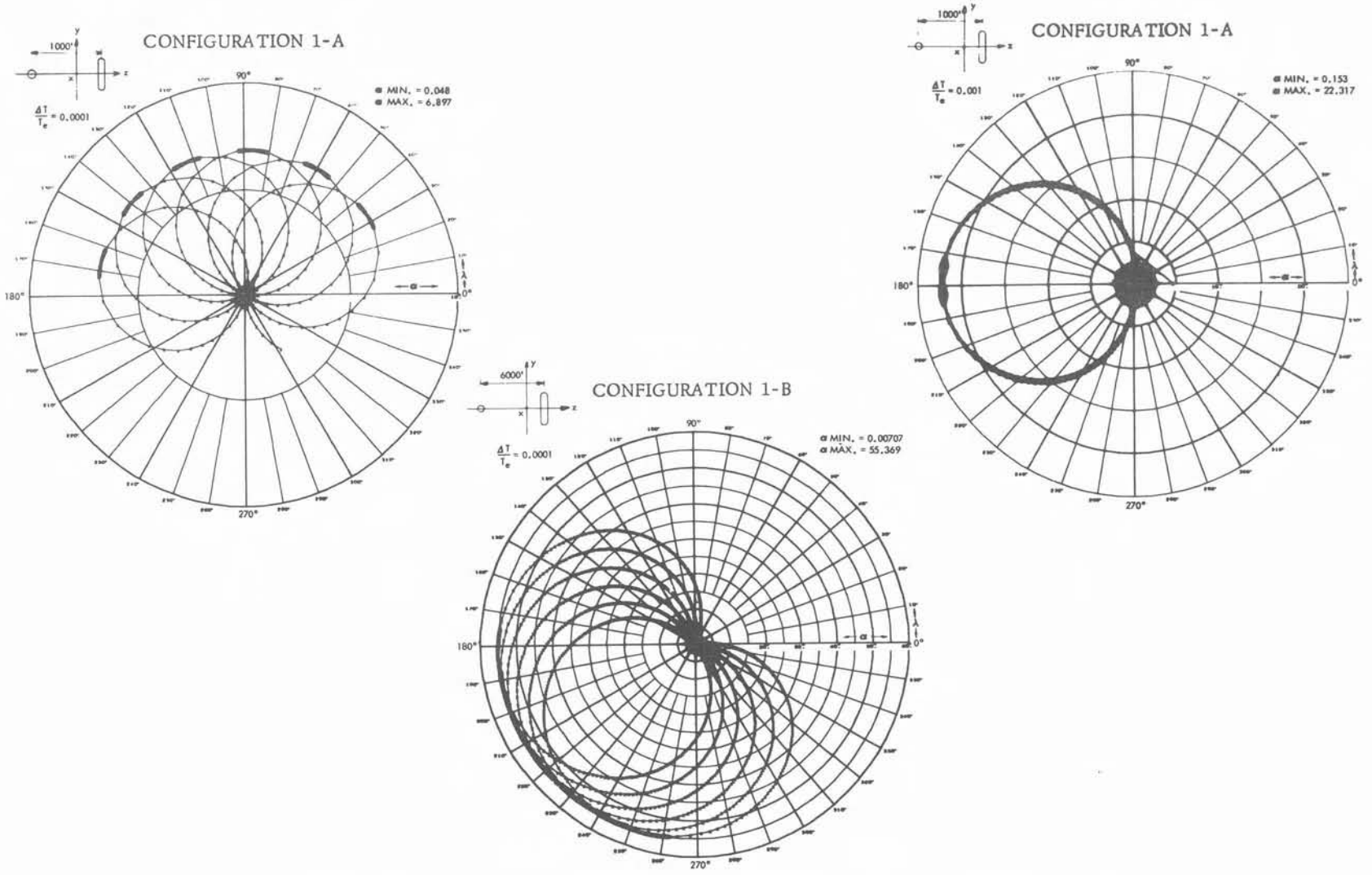

Figure 19. Rotational Stability of Spinning Elastic Bodies

For a smaller $\Delta T/T_e = 0.0001$, the angle α varies between α min = 0.0295 degrees and α max = 6.142 degrees. This verifies that the compartment-cable-counterweight configuration is a less than desirably stable configuration without effective damping devices.

The spinning cable-connected space station has a stable circular orbit, but the cable will oscillate under the influence of the gravitational gradient and will have a neutral stability. Stability depends upon the velocity - proportional damping device. For the gravitational gradient alone, only a small percentage of the critical damping factor is required. The spin rate of the configuration decreases gradually to a very small magnitude. Until the cable tension caused by spin is of the same order of magnitude as the tension caused by the gravitational gradient, the cable-connected configuration may not be stable.

However, physical and mathematical approximations have been assumed in the formulation of equations: 1) restriction of motion to the orbital plane, 2) a spherical earth, 3) neglect of forces other than the force of gravity, and 4) neglect of change of cable length in the derivation of lateral modes. If one or more of these approximations are corrected with rigor, the conclusions already drawn may change.

Consideration of these approximations reveals that if one is serious about the application of tension members to the connection of living modules of a space station, an extensive research program must be conducted in the future, with emphasis on the areas of three-dimensional cable dynamics, the cable material and its internal energy dissipating mechanism, the nonlinear phase of slackening cable, deployment and control problems, and many other problem areas.

15. Aeroelasticity Effects of Inflatables

Several new and different vehicles have been proposed for achieving re-entry and recovery from orbital, sub-orbital and super-orbital flight, (see Figure 20). Generally, a basic requirement of such vehicles is that they be capable of being folded, or stowed, so as to occupy a minimum of space until the time of deployment. They must also be light in weight in order to represent only a small fraction of the mission payload. Due to the flexibility of inflated booms and fabrics, and due to nonlinear characteristics and unknown properties of materials, the aeroelastic effects of inflatables are hard to ascertain. For control of the vehicle during deployment, maneuvering and landing, the interaction of cable vibration, vehicle movements, and flexibility of the inflatable structure should be well established. A concerted analytical effort and comprehensive laboratory and flight test programs are needed to assure reasonable results.

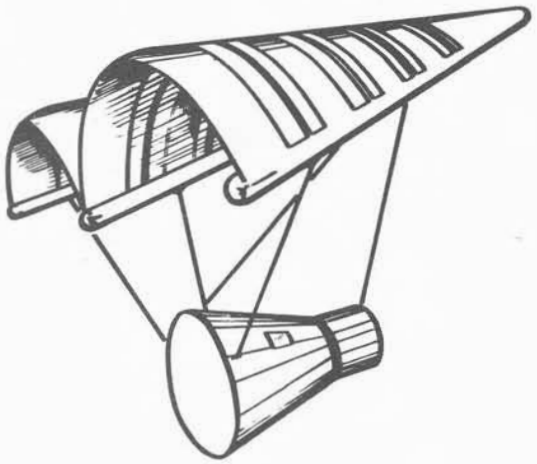

Figure 20. Paraglider with Gemini Capsule

16. Impact of Spacecraft in Water

Most spacecraft are of complicated configuration, consisting of sandwich or skin-stringer outer shells and pressurized inner shells with crew seats, in the case of manned craft. For decades the problem of impact of simple shells has been under investigation by many authors, with no remarkable results. The complex structural configuration, coupled with large degrees of freedom and the hydrodynamic interaction of waves with shells, increases the difficulty of predicting the stability of spacecraft and the dynamic loads associated with various landing speeds. Normally, naval architectural procedures were used to determine spacecraft flotation characteristics and statical stability. Fairly good correlation can be obtained for stability characteristics; however, structural response, load-time history, and vehicle integrity are hard to predict with purely analytical methods. A better understanding of the problem could be derived from a three-pronged approach:

1) additional theoretical study of shell impact and the hydrodynamic interaction of waves,
2) laboratory tests on components and models, and
3) semi-empirical formulae from full-scale tests.

Water impact testing of a "boilerplate" Apollo capsule is shown in Figure 21. S&ID is developing the Apollo Command Module under the direction of Manned Spacecraft Center.

Figure 21. Water Impact Test of "Boilerplate" Apollo

17. Impact of Spacecraft of Shell Configuration on Land

The two extremes of spacecraft landing environment are concrete and sand. A concrete landing surface is probably the easiest to simulate, analytically and experimentally, since the coefficient of friction is essentially constant and little or no kinetic energy is absorbed by the concrete. Landings in sand are complicated by the unknown contribution that sand makes to the total energy absorbed. During the alightment, the spacecraft will undergo compression, displacement, and shear through the surface. All of these factors contribute to the removal of energy from the moving body, along with the action of the spacecraft's energy absorption device. A typical device, employing air bags, is shown in Figure 22. As with impact on water, the prediction of dynamic loads in various parts of the complicated structure of a spacecraft impacting on land is a very difficult task. Comparison of typical analytical and experimental ground alightment acceleration histories are shown in Figure 23. Intense analytical studies, scale model and laboratory tests, and full-scale tests are necessary for a better understanding of the problem.

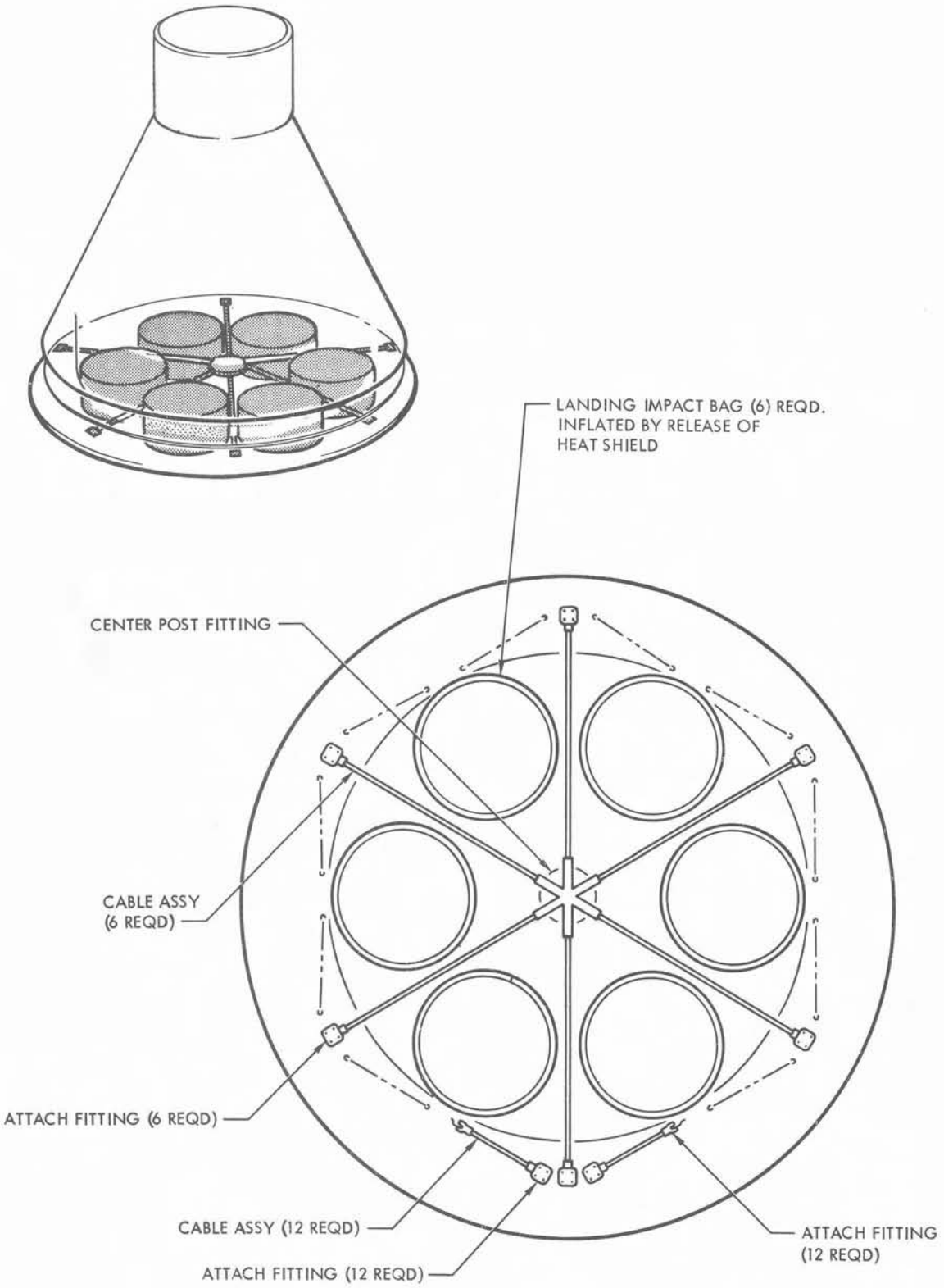

Figure 22. Air Bag Configuration - Six Bags with Cables

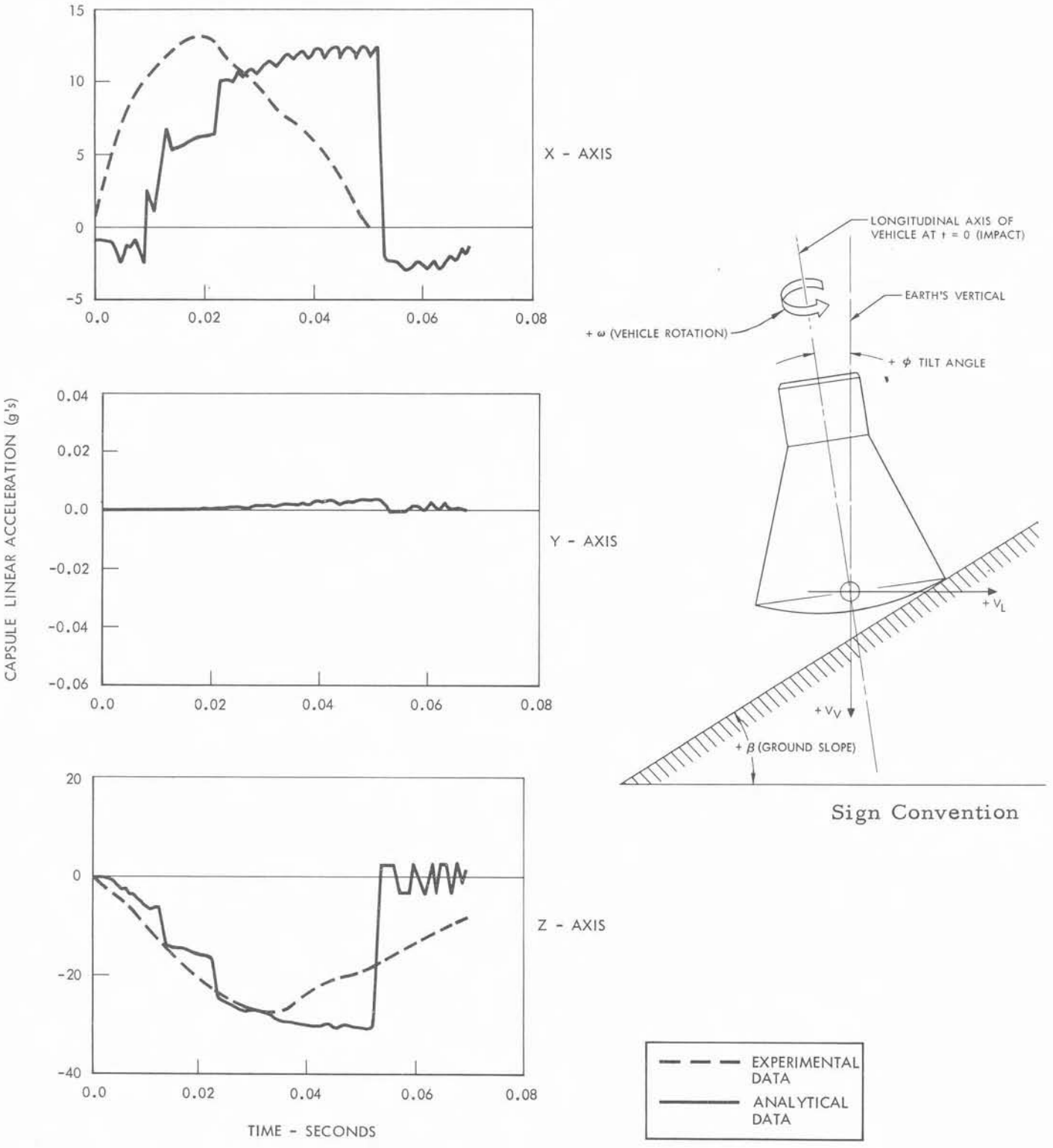

Figure 23. Comparison of Typical Analytical and Experimental Ground Alightment Acceleration Histories

18. Lunar Landing Structural Dynamics

Many theories of lunar geology have been postulated by many authors. The true characteristics of the lunar surface are still a matter of conjecture. The Ranger and Surveyor Programs are intended to provide a better understanding of the formation. The unknown factors of geology and topography, as well as the elastic and plastic effects of multiple-legged landings, make lunar landing dynamics a difficult task. Figure 24 shows a research model for use in dynamic analysis of legged-vehicle landings.

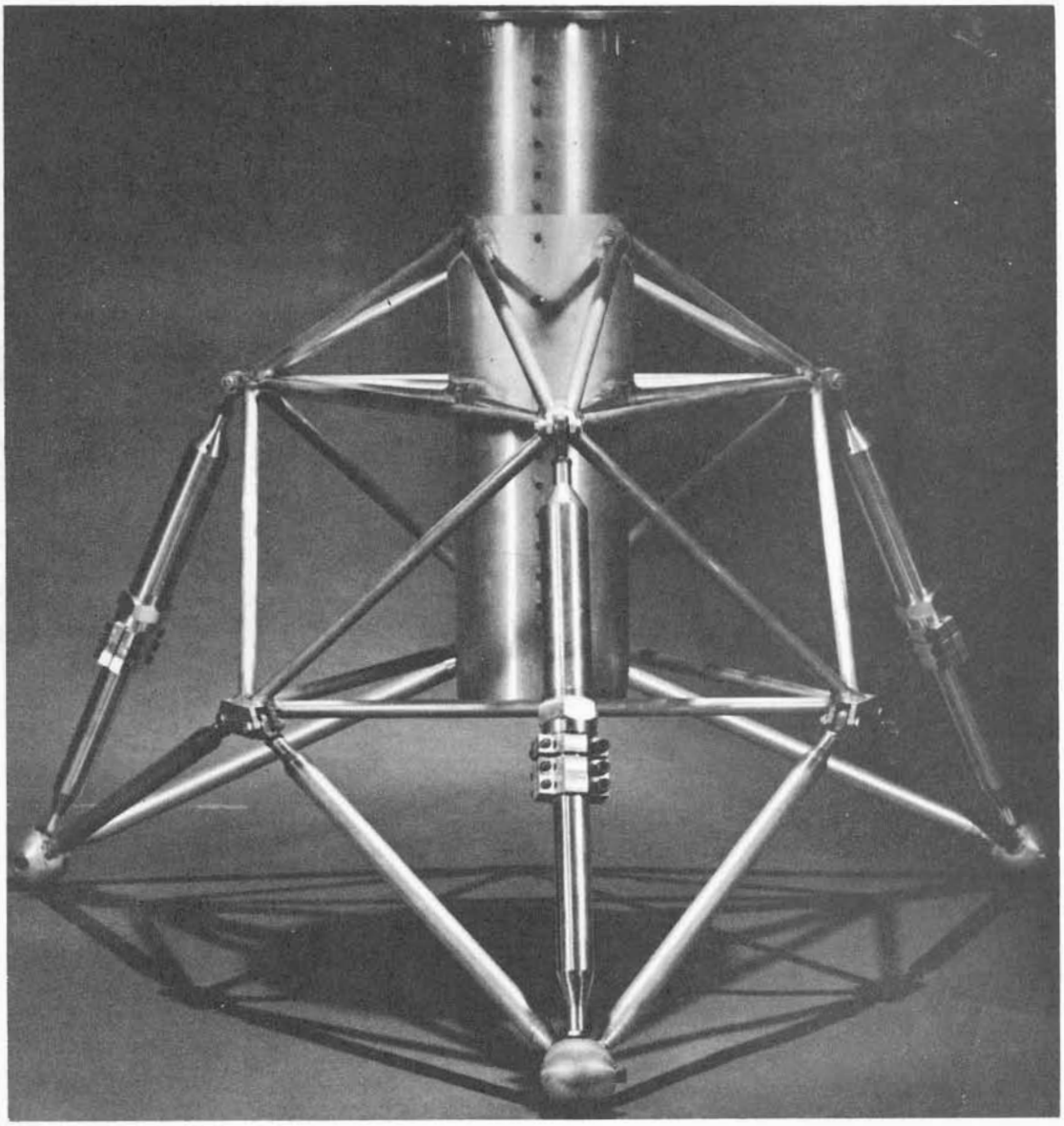

Figure 24. Frangible and Frictional Landing Model

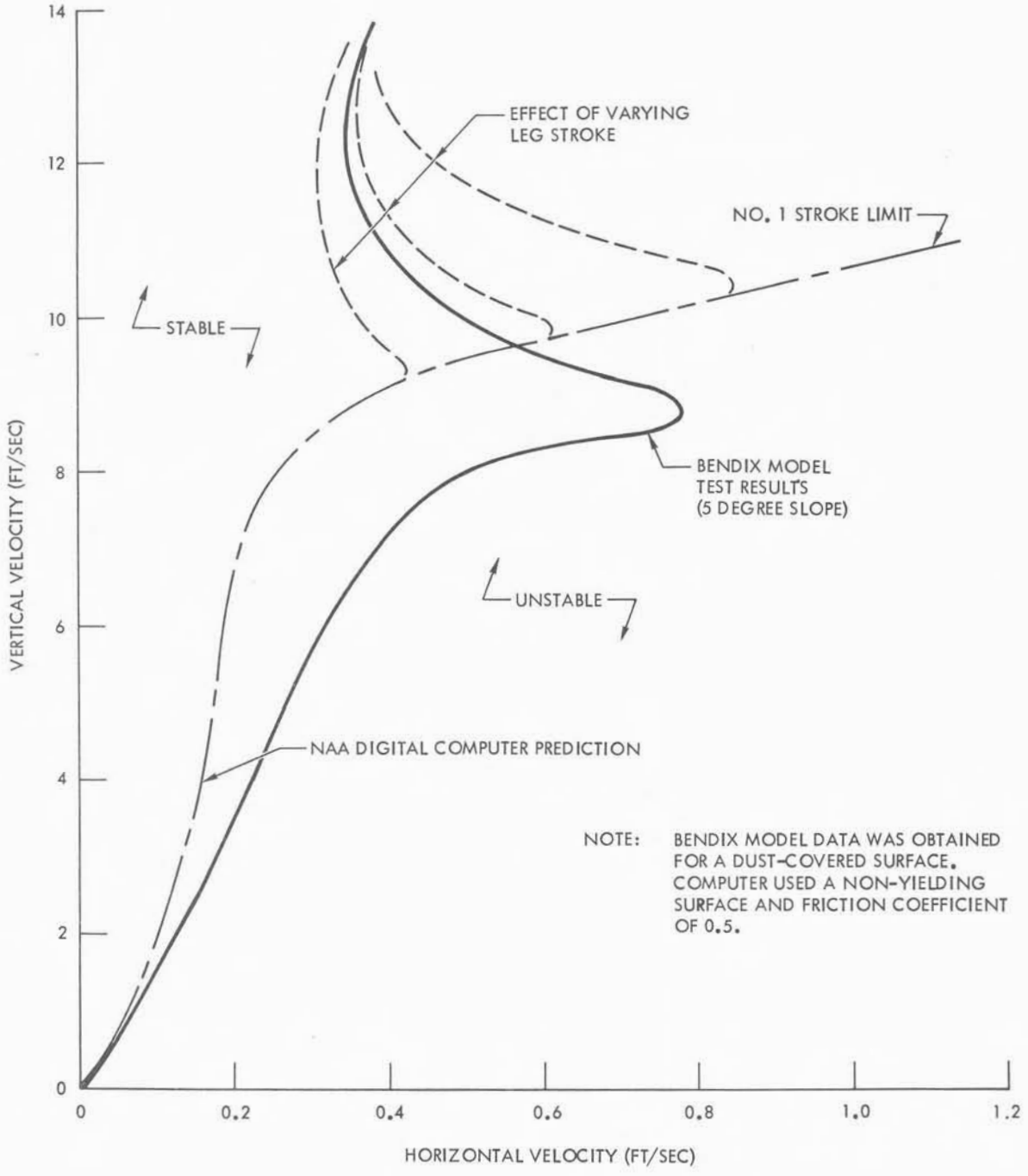

Figure 25. Analytical-Experimental Stability Correlation